

## AN EVALUATION OF SEDIMENTARY MOLYBDENUM AND IRON AS PROXIES FOR PORE FLUID PALEOREDOX CONDITIONS

DALTON S. HARDISTY<sup>\*\*\*\*†</sup>, TIMOTHY W. LYONS<sup>\*\*\*</sup>,  
NATASCHA RIEDINGER<sup>\*\*\*\*</sup>, TERRY T. ISSON<sup>§</sup>, JEREMY D. OWENS<sup>§§</sup>,  
ROBERT C. ALLER<sup>§§§</sup>, DANNY M. RYE<sup>§</sup>, NOAH J. PLANAVSKY<sup>§</sup>,  
CHRISTOPHER T. REINHARD<sup>§§§§</sup>, BEN C. GILL<sup>†</sup>, ANDREW L. MASTERSON<sup>††</sup>,  
DAN ASAEL<sup>§</sup>, and DAVID T. JOHNSTON<sup>†††</sup>

**ABSTRACT.** Iron speciation and trace metal proxies are commonly applied together in efforts to identify anoxic settings marked by the presence of free sulfide (euxinia) or dissolved iron (ferruginous) in the water column. Here, we use a literature compilation from modern localities to provide a new empirical evaluation of coupled Fe speciation and Mo concentrations as a proxy for pore water sulfide accumulation at non-euxinic localities. We also present new Fe speciation, Mo concentration, and S isotope data from the Friends of Anoxic Mud (FOAM) site in Long Island Sound, which is marked by pore water sulfide accumulation of up to 3 mM beneath oxygen-containing bottom waters. For the operationally defined Fe speciation scheme, ‘highly reactive’ Fe ( $Fe_{HR}$ ) is the sum of pyritized Fe ( $Fe_{py}$ ) and Fe dominantly present in oxide phases that is available to react with pore water sulfide to form pyrite. Observations from FOAM and elsewhere confirm that  $Fe_{py}/Fe_{HR}$  from non-euxinic sites is a generally reliable indicator of pore fluid redox, particularly the presence of pore water sulfide. Molybdenum (Mo) concentration data for anoxic continental margin sediments underlying oxic waters but with sulfidic pore fluids typically show authigenic Mo enrichments (2–25 ppm) that are elevated relative to the upper crust (1–2 ppm). However, compilations of Mo concentrations comparing sediments with and without sulfidic pore fluids underlying oxic and low oxygen (non-euxinic) water columns expose non-unique ranges for each, exposing false positives and false negatives. False positives are most frequently found in sediments from low oxygen water columns (for example, Peru Margin), where Mo concentration ranges can also overlap with values commonly found in modern euxinic settings. FOAM represents an example of a false negative, where, despite elevated pore water sulfide concentrations and evidence for active Fe and Mn redox cycling in FOAM sediments, sedimentary Mo concentrations show a homogenous vertical profile across 50 cm depth at 1 to 2 ppm. A diagenetic model for Mo provides evidence that muted authigenic enrichments are derived from elevated sedimentation rates. Consideration of a range of additional parameters, most prominently pore water Mo concentration, can replicate the ranges of most sedimentary Mo concentrations observed in modern non-euxinic settings. Together, the modern Mo and Fe data compilations and diagenetic model provide a framework for

\* Department of Earth and Environmental Sciences, Michigan State University, East Lansing, Michigan 48824, USA

\*\* Department of Geology and Geophysics, Woods Hole Oceanographic Institution, Woods Hole, Massachusetts 02543, USA

\*\*\* Department of Earth Sciences, University of California-Riverside, Riverside, California 92521, USA

\*\*\*\* Boone Pickens School of Geology, Oklahoma State University, Stillwater, Oklahoma 74075, USA

§ Department of Geology and Geophysics, Yale University, New Haven, Connecticut 06511, USA

§§ Department of Earth, Ocean and Atmospheric Science, National High Magnetic Field Laboratory, Florida State University, Tallahassee, Florida 32310, USA

§§§ School of Marine and Atmospheric Sciences, Stony Brook University, Stony Brook, New York 11794, USA

§§§§ School of Earth and Atmospheric Sciences, Georgia Institute of Technology, Atlanta, Georgia 30318, USA

† Department of Geosciences, Virginia Polytechnic and State University, Blacksburg, Virginia 24061, USA

†† Department of Earth and Planetary Sciences, Northwestern University, Evanston, Illinois 60208, USA

††† Department of Earth and Planetary Sciences, Harvard University, Cambridge, Massachusetts 02138, USA

† Corresponding author: dhardisty@whoi.edu

**identifying paleo-pore water sulfide accumulation in ancient settings and linked processes regulating seawater Mo and sulfate concentrations and delivery to sediments. Among other utilities, identifying ancient accumulation of sulfide in pore waters, particularly beneath oxic bottom waters, constrains the likelihood that those settings could have hosted organisms and ecosystems with thiotrophy at their foundations.**

Key words: paleoredox, iron speciation, molybdenum, pore water sulfide, Long Island Sound

#### INTRODUCTION

Iron speciation and molybdenum concentrations have been well calibrated in modern settings for recognizing end-member euxinic (anoxic and H<sub>2</sub>S-containing) and ferruginous (anoxic and iron-rich) settings in the geologic record (Bernier, 1970; Raiswell and others, 1988; Canfield and others, 1992; Canfield and others, 1996; Raiswell and Canfield, 1998; Poulton and Canfield, 2005, 2011; Lyons and Severmann, 2006; Algeo and Lyons, 2006; Raiswell and others, 2018). This past research has resulted in extensive application of these proxies toward an improved understanding of water column redox evolution and dynamics through time, including Phanerozoic ocean anoxic events (März and others, 2008; Gill and others, 2011), the Proterozoic (Poulton and others, 2004; Canfield and others, 2007; Scott and others, 2008; Li and others, 2010; Planavsky and others, 2011; Johnston and others, 2012; Sperling and others, 2015), and the Archean (Reinhard and others, 2009; Kendall and others, 2010; Scott and others, 2011). Beyond the recognition of ancient euxinic and ferruginous water columns, more recent research has provided a context for using Fe and Mo proxies to infer accumulation of sulfidic pore waters in ancient sediments, including those deposited beneath water columns lacking dissolved sulfide and Fe (Scott and Lyons, 2012; Sperling and others, 2015). Refined recognition of these conditions has important implications for the evolution of the marine sulfate reservoir and for interpretation of the geochemical impacts of sediment mixing induced by benthic infaunal communities through time (Canfield and Farquhar, 2009; Tarhan and others, 2015). Additionally, pore water sulfide has implications for bottom water habitability and the evolution of thiotrophy and associated symbiotic relationships among combined micro-/macrofaunal communities (Sperling and others, 2015; Tarhan and others, 2015). However, although a broad framework currently exists for understanding the conditions leading to Mo and Fe fixation in sulfidic sediments (see background), few studies have systematically evaluated proxy expressions from modern sediments to assess their potential as uniquely pore fluid indicators of paleoredox in ancient sediments.

Here, we specifically assess the paleoredox proxy potential of Fe speciation and Mo concentrations to recognize the presence or absence of pore water sulfide accumulation during early diagenesis from modern marine sediments underlying water columns without stable euxinia and a range of ambient oxygen concentrations. This endeavor is grounded in a broad context provided by compilations of Fe speciation and Mo concentrations from modern localities where water column and pore water redox conditions are well characterized. In addition, we present an original case study with Fe-speciation, Mo concentration, and S concentration and isotope data for sediments from the oxic FOAM (Friends of Anoxic Mud) site in Long Island Sound (LIS), USA, where sedimentary pore fluids are well-known to host elevated and persistent pore water sulfide concentrations. Previous studies of LIS, including the FOAM site, have been fundamental to the initial development of the Fe paleoredox proxies and a range of other sedimentary geochemical signatures (Aller and Cochran, 1976; Goldhaber and others, 1977; Benninger and others, 1979; Benoit and others,

1979; Aller, 1980a, 1980b; Krishnaswami and others, 1980; Westrich, ms, 1983; Berner and Westrich, 1985; Canfield, 1989; Canfield and Berner, 1987; Canfield and others, 1992; Canfield and Thamdrup, 1994; Raiswell and others, 1994; Raiswell and Canfield, 1998). We use a diagenetic model for Mo to provide constraints on the environmental factors that best explain the observed modern sediment concentration ranges and provide a context for interpreting non-euxinia related drivers of changes in Mo concentrations from ancient sediments.

#### BACKGROUND AND PROXY FRAMEWORK

##### *The Iron Proxies*

The utility of the Fe geochemical proxies is built on a foundation of extensive work on the reactivity of Fe minerals with dissolved sulfide in sedimentary environments (Berner, 1970; Raiswell and others, 1988; Canfield and others, 1992; Raiswell and others, 1994; Canfield and others, 1996; Raiswell and Canfield, 1998; Poulton and Canfield, 2005) and a well-developed understanding of syngenetic (water column) versus diagenetic pyrite formation (Canfield and others, 1996; Lyons, 1997; Wijsman and others, 2001; Lyons and others, 2003; Anderson and Raiswell, 2004; Raiswell and Anderson, 2005). The refined sequential extraction scheme of Poulton and Canfield (2005) is designed to target Fe phases, emphasizing carbonate-bound Fe, oxide Fe (dithionite extractable,  $Fe_{\text{dith}}$ ), and magnetite Fe (oxalate extractable,  $Fe_{\text{mag}}$ ), which all react with sulfide to form pyrite ( $Fe_{\text{py}}$ ) and Fe monosulfides (acid volatile sulfur,  $Fe_{\text{AVS}}$ ) on time scales relevant to early diagenesis (Canfield, 1989; Canfield and others, 1992; Canfield and others, 1996). These iron phases, when summed with pyrite, comprise the operationally defined 'highly reactive' Fe ( $Fe_{\text{HR}}$ ) pool.

Inputs of detrital  $Fe_{\text{HR}}$  into sediments permit the production of pyrite when exposed to sulfide, but typical lithogenic ratios of  $Fe_{\text{HR}}/Fe_{\text{T}} < 0.38$  and  $Fe_{\text{T}}/Al$  mass ratios  $\sim 0.5$  are maintained when anoxic (euxinic or ferruginous) conditions are not present in the water column (Raiswell and Canfield, 1998; Lyons and others, 2003; Lyons and Severmann, 2006). In contrast, if anoxia develops and persists in the water column, both  $Fe_{\text{HR}}/Fe_{\text{T}}$  and  $Fe_{\text{T}}/Al$  are elevated beyond these crustal baselines, and those enrichments are often used to infer ancient anoxia. According to one model, soluble Fe(II) generated during reductive dissolution of Fe-oxides along continental margins diffuses out of sediments, allowing enhanced delivery of  $Fe_{\text{HR}}$  through an 'Fe shuttle' to the deep basin where it is captured as syngenetic pyrite (Canfield and others, 1996; Lyons, 1997; Raiswell and Canfield, 1998; Wijsman and others, 2001; Anderson and Raiswell, 2004; Raiswell and Anderson, 2005; Lyons and Severmann, 2006; Severmann and others, 2008; Severmann and others, 2010; Scholz and others, 2014b). This 'extra' Fe is decoupled from the local delivery of silicate phases, including unreactive Fe fractions, with the net result of  $Fe_{\text{HR}}/Fe_{\text{T}} > 0.38$  (Raiswell and Canfield, 1998) and  $Fe_{\text{T}}/Al > 0.5$ . Under euxinic conditions, near complete reaction of the  $Fe_{\text{HR}}$  to form pyrite leads to  $Fe_{\text{py}}/Fe_{\text{HR}}$  ratios in excess of 0.7 to 0.8 (Poulton and others, 2004; März and others, 2008; Poulton and Canfield, 2011).

In sulfidic sediments underlying non-euxinic or ferruginous water column conditions, hence  $Fe_{\text{HR}}/Fe_{\text{T}} < 0.38$  and  $Fe_{\text{T}}/Al \sim 0.5$ , the  $Fe_{\text{py}}/Fe_{\text{HR}}$  ratio is anticipated to be  $> 0.7$ . This prediction is based on work from the Long Island Sound FOAM site (see FOAM background) where it was initially shown that pore water sulfide accumulation is preceded by the consumption of 'highly reactive' Fe minerals via reaction with sulfide to form pyrite (Canfield, 1989; Canfield and others, 1992). Sequential Fe extractions and associated  $Fe_{\text{py}}/Fe_{\text{HR}}$  of ancient shales have been applied previously to interpret pore water redox in ancient sediments (Sperling and others, 2015), but no study has evaluated the potential of  $Fe_{\text{py}}/Fe_{\text{HR}}$  from modern non-euxinic settings to uniquely indicate pore water sulfide accumulation—hence this study.

*Molybdenum Geochemistry*

Molybdenum is the most abundant transition metal in the modern ocean, with a near uniform concentration of  $\sim 104$  nM (Broecker and Peng, 1982; Emerson and Husted, 1991) and a relatively long residence time of  $\sim 450$  kyr (Miller and others, 2011). Molybdenum exists almost entirely as molybdate ( $\text{MoO}_4^{-2}$ ) under oxic conditions, delivered primarily from oxidative weathering of sulfide minerals (Miller and others, 2011). Molybdate has a strong affinity for sorption to Mn and Fe oxides, which is a significant pathway of Mo deposition in the modern, dominantly oxic ocean (Shimmield and Price, 1986; Barling and Anbar, 2004). In the absence of free sulfide in the water column and sediments, Mo buried with oxides will often diffuse back to the overlying water column following reductive dissolution of the oxides during sediment diagenesis (Shimmield and Price, 1986; Goldberg and others, 2012; Scott and Lyons, 2012), with the possibility of little to no authigenic sediment enrichment and thus concentrations near those characteristic of average continental crust ( $\sim 1$ – $2$  ppm).

Under sulfide-rich conditions, however, Mo is readily converted from  $\text{MoO}_4^{-2}$  to particle reactive thiomolybdate ( $\text{MoO}_{4-x}\text{S}_x^{-2}$ ; (Helz and others, 1996; Erickson and Helz, 2000; Zheng and others, 2000), which is buried in association with organic matter and pyrite (Algeo and Lyons, 2006; Chappaz and others, 2014; Dahl and others, 2017; Wagner and others, 2017). This relationship has particular importance when considering settings with sulfide restricted to the sediment pore fluids versus euxinic sites. In either case, if total dissolved sulfide concentrations exceed  $\sim 100$   $\mu\text{M}$  (with some sensitivity to ambient pH), quantitative sulfidization of  $\text{MoO}_4^{-2}$  to  $\text{MoS}_4^{-2}$  is expected (Helz and others, 1996; Erickson and Helz, 2000; Zheng and others, 2000; Helz and others, 2011). Molybdenum enrichments under euxinic water column conditions typically exceed the average continental crust value of approximately 1 to 2 ppm (Taylor and McLennan, 1995) by a significant margin—with sediment concentrations of up to hundreds of ppm (Scott and Lyons, 2012) and distinct relationships with the abundance of organic carbon in the sediments (Algeo and Lyons, 2006). In modern sulfidic sediments accumulating beneath an oxic water column, Mo delivered to the sediments—including that associated with oxide deposition and subsequent dissolution—is retained upon oxide dissolution via reaction with dissolved sulfide, among other possibilities (Scholz and others, 2017). Rather than diffusing back to the overlying water column, this Mo is sequestered with organic matter and/or pyrite in the subsurface layers (Helz and others, 1996; Erickson and Helz, 2000; Helz and others, 2011; Chappaz and others, 2014; Dahl and others, 2017; Wagner and others, 2017). A recent survey of Mo concentrations from non-euxinic settings with sulfidic pore fluids suggests that authigenic enrichments rarely exceed 25 ppm, with most of these settings having enrichments below 10 ppm (Scott and Lyons, 2012). A new diagenetic model, the new FOAM data, and the literature data compilation presented here is intended to extend the proxy potential of Mo concentrations to differentiate settings with pore fluid sulfide accumulation from those lacking sulfide or with sulfide also present in the water column.

*FOAM—The Historical Context*

Past studies of FOAM and several nearby locations in Long Island Sound must get credit for giving rise to the Fe-based paleoredox proxies—specifically, degree of pyritization (DOP),  $\text{Fe}_{\text{HR}}/\text{Fe}_{\text{T}}$ , and  $\text{Fe}_{\text{py}}/\text{Fe}_{\text{HR}}$ . The water column is oxygenated at each of these localities (Lee and Lwiza, 2005; Lee and Lwiza, 2008; Wallace and others, 2014), and sedimentary sulfide concentrations range from 2 to 6 mM at FOAM and the adjacent study sites characterized by high rates of sulfate reduction (Goldhaber and others, 1977; Westrich, ms, 1983; Canfield, 1989; Canfield and others, 1992). Studies at

FOAM demonstrate that DOP data from sediments with sulfidic pore waters, but underlying oxic water columns, are clearly distinguishable from those of euxinic water column settings. Specifically, DOP values from FOAM and nearby LIS sediments do not exceed  $\sim 0.4$  (Berner, 1970; Canfield and others, 1992; Raiswell and Canfield, 1998), which are readily distinguished from the values of  $>0.7$  found in sediments underlying euxinic water columns (Raiswell and others, 1988). Similarly, comparisons of  $\text{Fe}_{\text{HR}}/\text{Fe}_{\text{T}}$  data from FOAM and other modern oxic localities to sediments in modern euxinic basins established the  $\text{Fe}_{\text{HR}}/\text{Fe}_{\text{T}}$  threshold of  $\sim 0.38$  now used widely to identify ancient euxinic and ferruginous water columns (Raiswell and Canfield, 1998). These same studies also demonstrated the reactivity of common Fe minerals—ferrihydrite, lepidocrocite, goethite, hematite, magnetite—towards sulfide to form pyrite. Concurrently, other Fe minerals (for example, sheet silicates) were found instead to react with sulfide on much longer timescales well beyond those of early diagenesis (Canfield and Berner, 1987; Canfield, 1989; Canfield and others, 1992; Raiswell and others, 1994).

The intermediate DOP values at FOAM, despite high and persistent levels of pore water sulfide, set the stage of a deeper exploration of reactive iron (reviewed in Lyons and Severmann, 2006) and the mechanistic underpinnings of the Fe-based paleoredox proxies—leading ultimately to the now widely used sequential extraction protocol (Poulton and Canfield, 2005). This refined approach targets the ‘highly reactive’ Fe phases described above. Collectively, data from FOAM and the modern Black Sea (Canfield and others, 1996) exposed the need for ‘extra’ highly reactive Fe in euxinic settings to explain observations of elevated DOP and  $\text{Fe}_{\text{HR}}/\text{Fe}_{\text{T}}$  (Canfield and others, 1996; Lyons, 1997; Raiswell and Canfield, 1998; Wijsman and others, 2001; Anderson and Raiswell, 2004; Raiswell and Anderson, 2005; Lyons and Severmann, 2006; Severmann and others, 2008; Severmann and others, 2010; Scholz and others, 2014b). Our study, however, is the first report of  $\text{Fe}_{\text{HR}}/\text{Fe}_{\text{T}}$  data from FOAM using the expanded suite of Fe extractions (Poulton and Canfield, 2005) and to specifically report  $\text{Fe}_{\text{py}}/\text{Fe}_{\text{HR}}$  for this location. Comparisons with previous studies are possible, however, since data for  $\text{Fe}_{\text{dih}}$ ,  $\text{Fe}_{\text{py}}$ , and  $\text{Fe}_{\text{AVS}}$  were already available for the upper 12 cm of FOAM (Berner and Canfield, 1989; Raiswell and Canfield, 1998). Those studies yielded  $\text{Fe}_{\text{HR}}/\text{Fe}_{\text{T}}$  ratios of 0.2 to 0.3 and  $\text{Fe}_{\text{py}}/\text{Fe}_{\text{HR}}$  values approaching 0.8 in the presence of high concentrations of pore water sulfide.

Beyond Fe proxy development and calibration, the FOAM site has been the focus of numerous, now classic studies on sulfate reduction and sulfur disproportionation (Goldhaber and others, 1977; Westrich, ms, 1983; Canfield and Thamdrup, 1994), bioturbation (Aller, 1980a, 1980b; Berner and Westrich, 1985), and sedimentation rates (Krishnaswami and others, 1984), among other topics (Aller and Cochran, 1976; Benninger and others, 1979; Benoit and others, 1979; Krishnaswami and others, 1980).

Sedimentation rates at FOAM and adjacent study sites have been found to range from 0.03 to 0.3 cm/yr (Goldhaber and others, 1977; Krishnaswami and others, 1984). The presence of bioturbation and infaunal irrigation to depths of 8 to 10 cm (Goldhaber and others, 1977) has left the upper 4 cm of the sediment well mixed (Aller, 1980a; Krishnaswami and others, 1984). The activities of these burrowing organisms have been documented to change on seasonal time scales (Goldhaber and others, 1977; Aller, 1980a, 1980b), thus enhancing infaunal irrigation of sulfate to the sediments in the summer compared to winter and creating distinct differences in the depth of sulfide accumulation from winter to summer. Bioturbation is the dominant transport mechanism in the summer, and diffusion dominates during the winter (Goldhaber and others, 1977). Previous FOAM studies have suggested that diagenetic processes are not in steady state in the upper  $\sim 10$  cm, where active bioturbation and maximum seasonal temperature variation occur, and are approximately at steady state

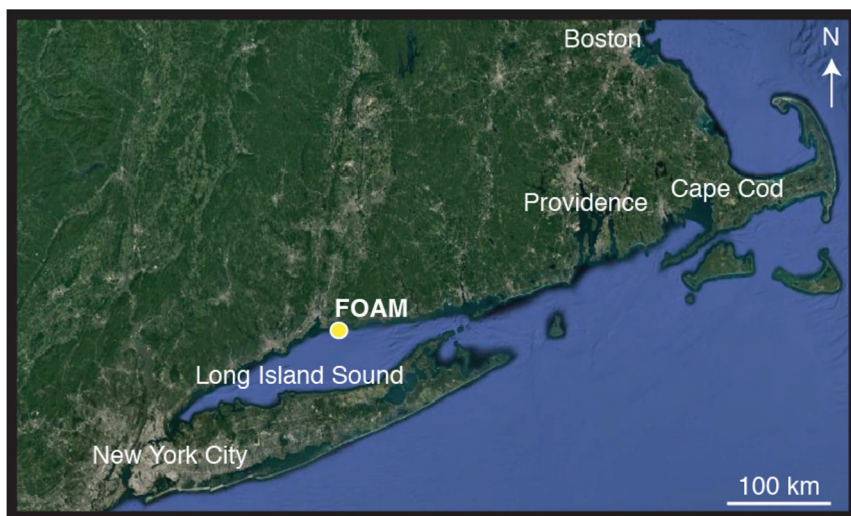


Fig. 1. Map showing FOAM location. Image is taken from Google Earth.

at depth (Aller, 1980a, 1980b; Westrich, ms, 1983; Boudreau and Canfield, 1988). Occasional dredging of portions of the Sound may cause sediment reworking, but no direct impacts of dredging have been observed at FOAM.

#### METHODS

Our FOAM core was collected in October 2010 using a modified piston-gravity corer (fig. 1). The site is located at  $41^{\circ}14'26.82''\text{N}$ ,  $72^{\circ}44'44.78''\text{W}$  at a water depth of approximately 10 m. Cores were sectioned into 1 to 2 cm intervals within 2 hours of collection, and the sediment was transferred into 50 mL centrifuge tubes. Pore waters were extracted within an  $\text{N}_2$ -flushed glove bag using rhizons within several hours of core retrieval (Seeberg-Elverfeldt and others, 2005). Pore water subsamples for hydrogen sulfide ( $\Sigma\text{H}_2\text{S}$ ) were fixed with zinc acetate, while subsamples for metal analysis were acidified with trace metal grade HCl. Residual sediment samples were sealed and frozen immediately, minimizing oxidation.

Pore water  $\Sigma\text{H}_2\text{S}$  concentrations were measured using the methylene blue method (Cline, 1969). Sulfate concentrations were determined by suppressed ion chromatography with conductivity detection (ICS-2000, AS11 column; Dionex) at the Stable Isotope Geobiology Laboratory at Harvard University. Pore water concentrations of Mn, Fe, and Mo were measured via inductively coupled plasma-mass spectrometry (ICP-MS; Agilent 7500ce) at the University of California Riverside. Sample replicates yielded standard deviations  $<5$  percent for Mn, Fe, and Mo.

Acid volatile sulfur (AVS) and chromium reducible sulfur (CRS) were determined sequentially using freshly thawed frozen samples and quantified by iodometric titration (Canfield and others, 1986). Recoveries of sulfur for pure pyrite standards averaged  $86 \pm 9.2$  percent of the expected amount ( $n = 8$ ); however, duplicate analyses of FOAM samples revealed better reproducibility. To determine the degree of pyritization (DOP) for FOAM sediments, Fe was extracted using the boiling HCl method of Berner (1970) and Raiswell and others (1988). Following from previous work (Berner, 1970; Raiswell and others, 1988), DOP was calculated as  $\text{Fe}_{\text{py}} / (\text{Fe}_{\text{py}} + \text{Fe}_{\text{HCl}})$ .

Samples with the bulk of pore water previously extracted but still wet were thawed and weighed for determination of Fe speciation using a modified version of the

sequential Fe extraction of Poulton and Canfield (2005). An ascorbate step targeting ferrihydrite (Ferdeman, ms, 1988; Kostka and Luther, 1994; Raiswell and others, 2010), or  $\text{Fe}_{\text{asc}}$ , was added and replaced a sodium acetate extraction that targets carbonate-bound Fe given the unlikelihood of Fe carbonate precipitation in these sulfide-rich sediments. To minimize oxidation of Fe sulfide phases during the extraction procedures, the solutions were bubbled with  $\text{N}_2$  gas prior to extraction, and the headspace extraction vials were filled with  $\text{N}_2$  gas and sealed throughout the extractions. Replicate samples yielded precisions of <7 percent for  $\text{Fe}_{\text{asc}}$ ,  $\text{Fe}_{\text{dith}}$ , and  $\text{Fe}_{\text{mag}}$ . All iron phase values are reported on dry sediment basis corrected for water contents. Combined,  $\text{Fe}_{\text{py}}$ ,  $\text{Fe}_{\text{AVS}}$ ,  $\text{Fe}_{\text{asc}}$ ,  $\text{Fe}_{\text{dith}}$ , and  $\text{Fe}_{\text{mag}}$  represent the total 'highly reactive' Fe pool ( $\text{Fe}_{\text{HR}}$ ).

FOAM sediment samples were dried and then homogenized via mortar and pestle after removal of visible shell material. Total carbon was measured using an Eltra CS-500 carbon-sulfur analyzer. Total inorganic carbon was determined by measuring  $\text{CO}_2$  liberated after addition of 2.5 N HCl. Total organic carbon (TOC) was determined as the difference between total carbon and total inorganic carbon.

Bulk concentrations of Fe, Mn, Al, and Mo were determined using a total digestion of ashed samples (450 °C) in trace metal grade  $\text{HF}:\text{HNO}_3:\text{HCl}$ . Contents of Fe, Mn, Al, and Mo were measured using an Agilent 7500ce ICP-MS at the University of California-Riverside. Repeated analyses of USGS reference material SDO-1 were included to assess accuracy and precision, with all elements analyzed in this study falling within the reported ranges. The SDO-1 standard contains elevated concentrations of each of the elements of interest relative to FOAM samples and was therefore diluted during ICP-MS analysis to mimic the concentration range observed at FOAM. Digestion and analysis of duplicate and triplicate FOAM sediment samples revealed standard deviations ( $1\sigma$ ) of <0.1 weight percent for Al, Mn, and Fe and <0.2 ppm for Mo.

For the sake of comparison to past studies, we also include previously unpublished S isotope data from FOAM. The FOAM-1 core was collected in August 1974 and sectioned in 1 to 2 cm intervals under  $\text{N}_2$  in a glove bag within ~12 hours of collection. Pore waters were extracted by squeezing and filtered (Kalil and Goldhaber, 1973). Additional details can be found in Aller (1980a, 1980b).

To determine the isotopic composition of pore water sulfate in FOAM-1, pore water samples were diluted with ~70 mL distilled water, acidified with HCl, and heated.  $\text{BaSO}_4$  was precipitated following addition of  $\text{BaCl}_2$  (10% w/v). The acid volatile sulfur was extracted immediately following sample collection by reaction with cold 12 N HCl and the resulting  $\text{H}_2\text{S}$  was stripped with  $\text{N}_2$  and precipitated as  $\text{Ag}_2\text{S}$  in a  $\text{AgNO}_3$  trap (Aller, 1980a, 1980b).  $\text{BaSO}_4$  and  $\text{Ag}_2\text{S}$  were combusted to  $\text{SO}_2$  ( $\text{Ag}_2\text{S}$  by the cupric oxide method), and the sulfur isotope compositions were measured via a Nuclide 6–60 isotope ratio mass spectrometer at Yale University. For both  $\text{SO}_4^{2-}$  and AVS, the sulfur isotope data are presented in conventional delta notation ( $\delta^{34}\text{S}$ ) in permil (‰) relative to the Vienna Canyon Diablo Troilite (VCDT) standard and equation 1 below, which also applies to  $\delta^{33}\text{S}$ . Park City pyrite, a synthetic ZnS, and a synthetic PbS were used as secondary standards. Standard deviations ( $1\sigma$ ) for the analyses of secondary standards and duplicate samples were less than 0.1 permil.

$$\delta^{3X}\text{S} = [({}^{3X}\text{S}/{}^{32}\text{S})_{\text{sample}}/({}^{3X}\text{S}/{}^{32}\text{S})_{\text{standard}} - 1] \times 1000 \quad (1)$$

For the 2010 FOAM core, sulfur isotope analyses were performed at the Stable Isotope Geobiology Laboratory at Harvard University. Minor isotopes were measured via fluorination of  $\text{Ag}_2\text{S}$ , as shown below in equation 2. For sulfate, the samples are first reduced to  $\text{Ag}_2\text{S}$  with a mixture of hydriodic acid (HI), hypophosphorous acid ( $\text{H}_3\text{PO}_4$ ), and hydrochloric acid (HCl) at ~90 °C for 3 hours (Forrest and Newman, 1977; Johnston and others, 2007). Powdered  $\text{Ag}_2\text{S}$  samples were fluorinated at 300 °C

in an  $F_2$  atmosphere at  $10\times$  stoichiometric excess. Product  $SF_6$  was cryogenically and chromatographically purified and analyzed on a ThermoFinnigan 253 in Dual Inlet mode. Repeated analyses of standards IAEA-S1, S2, S3 yielded a reproducibility of  $\pm 0.2$  permil and  $\pm 0.006$  permil for  $\delta^{34}S$  and  $\Delta^{33}S$ , respectively. Samples are reported versus VCDT, which is calibrated from the long-term running average of IAEA-S1 versus the working standard gas at Harvard University.

$$\Delta^{33}S = \delta^{33}S - [(\delta^{34}S/1000 + 1)^{0.515} - 1] \times 1000 \quad (2)$$

#### RESULTS

We compiled literature data (figs. 2 and 3) that includes new data and earlier results from FOAM, Fe speciation from diverse modern settings ( $n = 1068$ ), and Mo concentrations from modern non-euxinic settings ( $n = 1421$ ). All citations are given in the respective figure captions. For both Fe speciation and Mo concentrations, 'oxic' is defined as settings with  $>15 \mu M O_2$ , and low oxygen conditions are defined as having  $<15 \mu M O_2$  but without persistent sulfide accumulation in the water column. For Mo, data from the Namibian Shelf are included in the low oxygen settings. In some cases, these low oxygen settings, such as the Peru Margin, are reported to have transient water column sulfide plumes (Scholz and others, 2016). We distinguish between data associated with dissolved hydrogen sulfide in the pore waters and pore waters with either dissolved sulfide below detection or appreciable dissolved Fe, which implies negligible sulfide. When available, the compiled  $Fe_{py}/Fe_{HR}$  data include iron associated with acid-volatile sulfide (AVS or 'FeS', the iron monosulfide precursors to pyrite formation). In figure 3, intervals with Mo associated with surface Mn enrichments ( $>2$  wt. % Mn in most cases) are not included.

Our pore water sulfide concentrations at FOAM are near 3 mM, which are within the range of concentrations previously observed ( $\sim 6$  mM; Goldhaber and others, 1977; Canfield and others, 1992), with measureable sulfide accumulation limited to depths of approximately 8 cm and greater (fig. 4A). Consistent with the down core increase in sulfide, pore water sulfate concentrations decrease with depth (fig. 4A). The TOC content ranges from 0.5 to 2.0 weight percent (fig. 4B). Pyrite is observed at all depths (fig. 4C) and is consistent with previously reported ranges at FOAM (Canfield, 1989; Canfield and others, 1992; Raiswell and Canfield, 1998). AVS was not detected in this study. Because some AVS has been reported from past FOAM studies (Aller, 1980b; Canfield, 1989; Canfield and others, 1992; Raiswell and Canfield, 1998), it may be missing in our samples due to oxidation. Sulfur isotope data ( $^{32}S$ ,  $^{33}S$ , and  $^{34}S$ ) for pyrite, acid volatile sulfide, and sulfate are shown for both the FOAM-1 (1974) and FOAM 2010 cores (fig. 4D) and are remarkably similar despite collection separated by nearly 40 years. For the minor sulfur isotopes (fig. 4E), the data mimic previous observations from similar sites (Johnston and others, 2008), with sulfate showing increasing  $\Delta^{33}S$  in parallel with  $\delta^{34}S$  increases. Sulfide  $\Delta^{33}S$  compositions are also enriched (averaging 0.16‰). Sulfur isotope data are shown in tables 1 and 2.

Results for individual Fe fractions are shown in table 3 and figure 5. Dissolved pore water Fe concentrations peak in the upper 4 cm, rising from 4.24  $\mu M$  at 0.5 cm to 6.29  $\mu M$  at 2 cm, before decreasing to 0.94  $\mu M$  at 10 cm (fig. 5A). These dissolved Fe values are notably similar to autumn cores from previous studies at FOAM (Aller, 1980b). Dithionite Fe is the most abundant measured highly reactive Fe fraction in the upper 10 cm other than pyrite, peaking at 0.14 weight percent (fig. 5B), while other Fe fractions are negligible (table 3). Calculated values for DOP are mostly near 0.4,  $Fe_T/Al$  ratios are approximately 0.5, and  $Fe_{HR}/Fe_T$  remains  $<0.38$  (figs. 5C and 5D). Ratios of  $Fe_{py}/Fe_{HR}$  ratios decline in the upper 5 cm of the core from 0.86 to 0.55 and are persistently  $>0.8$  starting at 8 cm (fig. 5D). Our values for  $Fe_T/Al$ ,  $Fe_{HR}/Fe_T$ ,



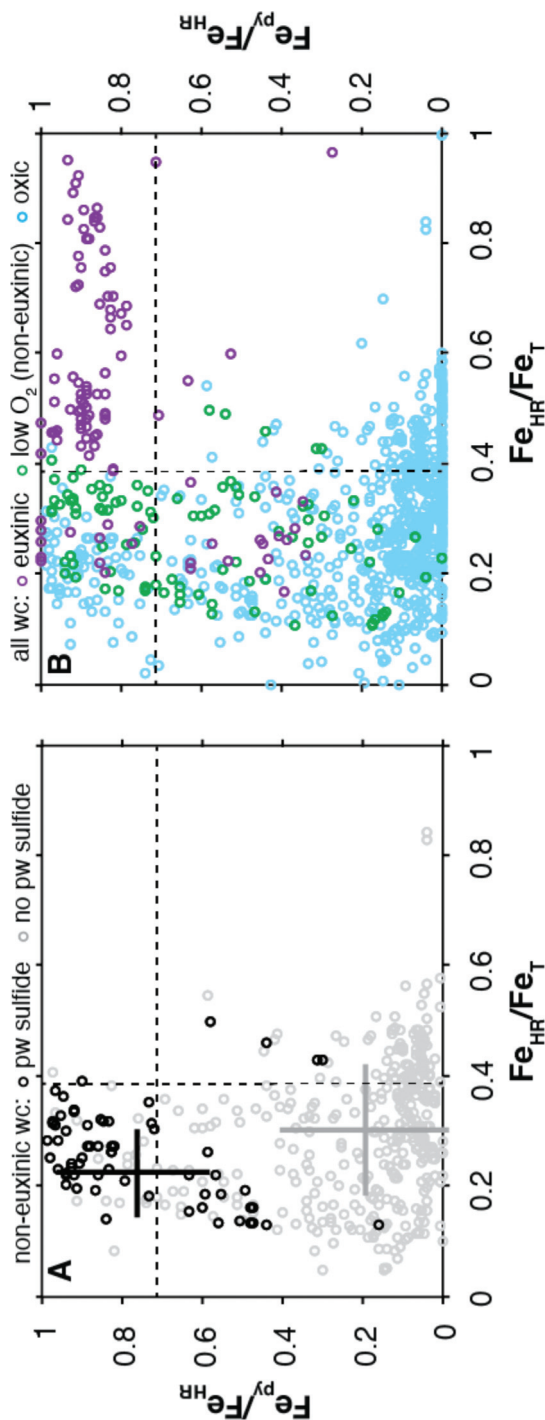


Fig. 2. Compilation of Fe speciation data from modern sediments. (A) Non-euxinic water columns with (Canfield, 1989; Scholz and others, 2014b; Raven and others, 2016; Riedinger and others, 2017) and without (Canfield, 1989; Wijsman and others, 2001; Aller and others, 2004; Goldberg and others, 2012; Scholz and others, 2014b; Wehrmann and others, 2014; Henkel and others, 2016; Riedinger and others, 2017) pore water sulfide in the host sediments. (B) Euxinic (Raiswell and Canfield, 1998; Wijsman and others, 2001; Lyons and others, 2003), low oxygen (Raiswell and Canfield, 1998; Scholz and others, 2014b; Raven and others, 2016), and oxic water columns (Canfield, 1989; Raiswell and Canfield, 1998; Aller and others, 2004; Goldberg and others, 2012; März and others, 2012; Zhu and others, 2012; Aquilina and others, 2014; Scholz and others, 2014b; Wehrmann and others, 2014; Peketi and others, 2015; Zhu and others, 2015; Henkel and others, 2016; Riedinger and others, 2017). Low oxygen is defined as  $<15 \mu\text{M O}_2$  but lacking detected sulfide. Notably, the 'highly reactive' Fe is determined differently between the publications, including the sequential extraction of Poulton and Canfield (2005), its predecessors (for example, Raiswell and Canfield, 1998; Aller and others, 2004), and other modifications (for example, Raven and others, 2016). When available,  $Fe_{py}/Fe_{HR}$  includes iron from the acid volatile S extraction in the numerator. The horizontal line represents the suggested boundary for oxic water column conditions for modern sediments, 0.38 (Canfield and Raiswell, 1998). The vertical line represents the  $Fe_{py}/Fe_{HR}$  boundary for indication of sulfide accumulation of 0.7, which is discussed in the main text. The solid bars represent  $\pm 1\sigma$  of the respective data.

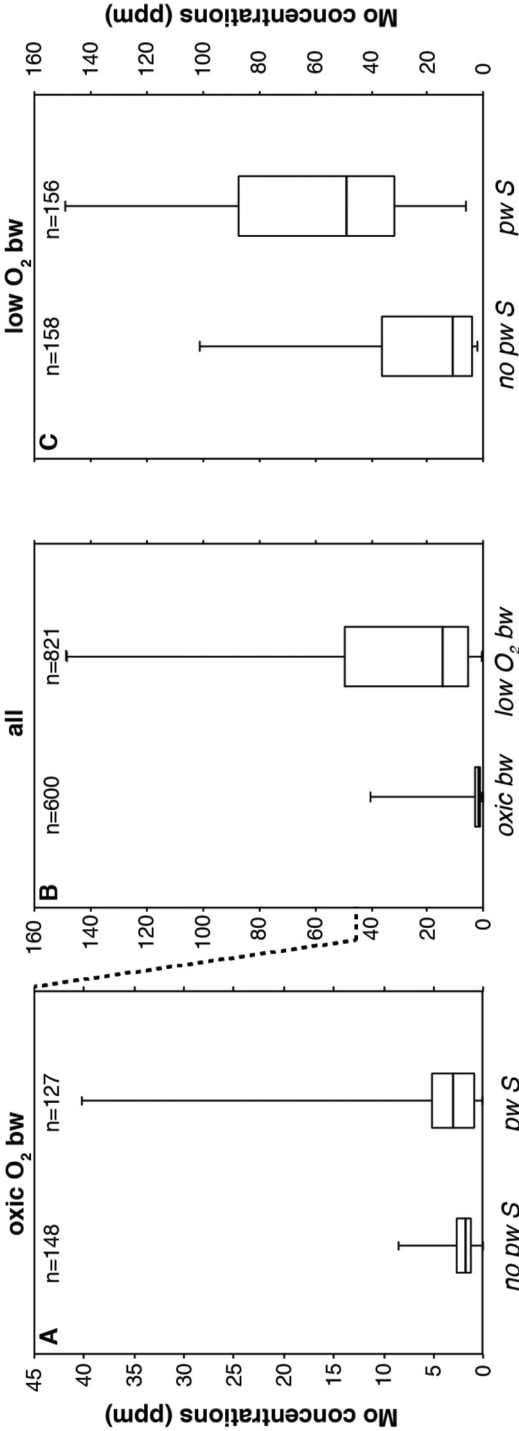


Fig. 3. Box and whisker plots comparing sedimentary Mo concentrations from: (A) Oxic water column settings with (Malcolm, 1985; Pedersen, 1985; Morford and others, 2007; Poulson Brucker and others, 2009) and without (Zheng and others, 2000; Böning and others, 2004; Morford and others, 2009; Poulson Brucker and others, 2009; Scholz and others, 2011; Goldberg and others, 2012) appreciable pore water sulfide concentrations. Intervals where Mo is associated with Mn enrichments (>2 wt. % Mn in most cases) are not included. Note the difference in scale in part A relative to B and C. (B) Oxic (Malcolm, 1985; Pedersen, 1985; Shimmield and Price, 1986; Morford and Emerson, 1999; Zheng and others, 2000; Böning and others, 2004; Sundby and others, 2004; McManus and others, 2006; Poulson and others, 2006; Morford and others, 2007; Poulson Brucker and others, 2009; Morford and others, 2009; Scholz and others, 2011; Goldberg and others, 2012) and low oxygen water columns (Brongersma-Sanders and others, 1980; Calvert and Price, 1983; Morford and Emerson, 1999; Zheng and others, 2000; Nameroff and others, 2002; Böning and others, 2004; McManus and others, 2006; Poulson and others, 2006; Poulson Brucker and others, 2009; Scholz and others, 2011) — defined as <15  $\mu\text{M O}_2$  but lacking dissolved sulfide. (C) Low oxygen water column sites with (Zheng and others, 2000; Poulson Brucker and others, 2004; Poulson Brucker and others, 2009; Scholz and others, 2011) and without (Zheng and others, 2000; Nameroff and others, 2002; Scholz and others, 2011) appreciable sulfide concentrations in the pore waters. A lack of appreciable sulfide is defined by sulfide measured but below detection, or sulfide not measured but with elevated dissolved Fe concentrations.

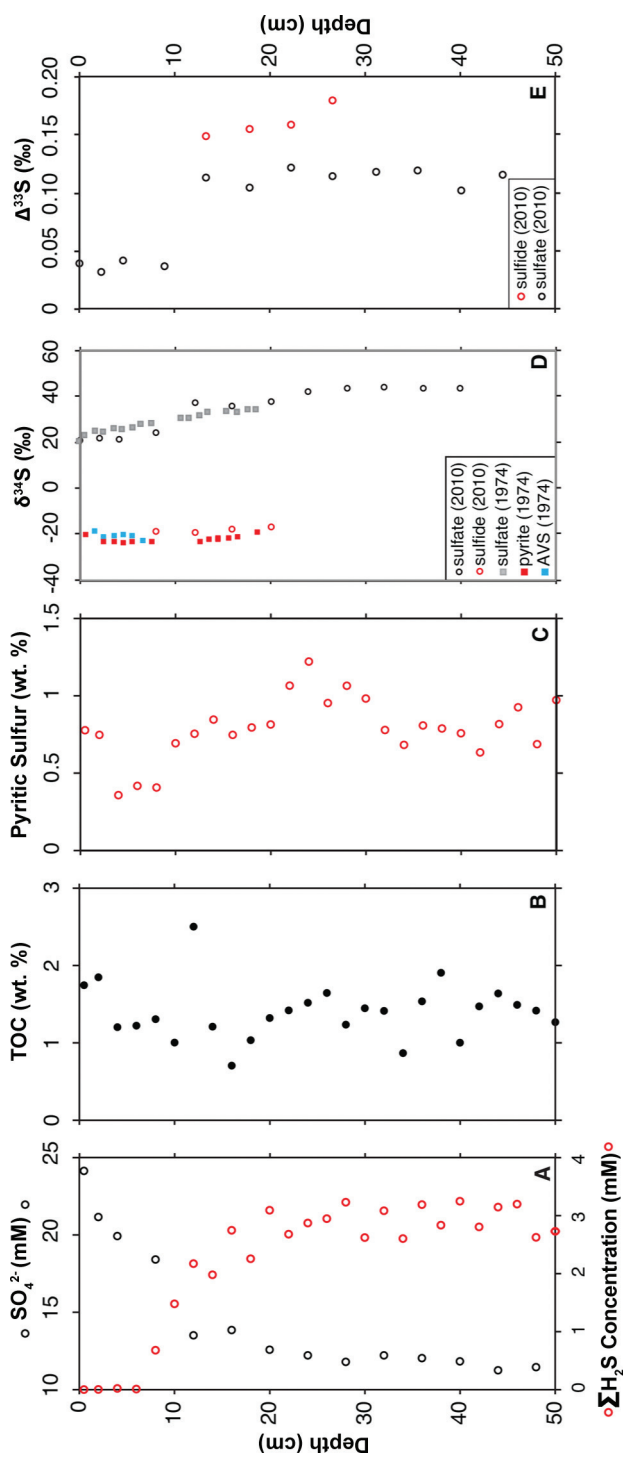


Fig. 4. FOAM concentration profiles for (A) pore water sulfate and hydrogen sulfide, (B) total organic carbon (TOC), and (C) weight percent sulfur in pyrite. Also included are isotope compositions of (D) <sup>34</sup>S (δ<sup>34</sup>S) of sulfate and dissolved sulfide and (E) <sup>33</sup>S (Δ<sup>33</sup>S) for sulfate and dissolved sulfide. In part D, data are shown from both the cores utilized for measurement in A, B, C, E of this figure (2010 core) and previously unpublished data from core FOAM-1 (Aller 1980a, 1980b). Sulfur isotope data are shown in tables 1 and 2.

TABLE 1  
Sulfur isotope values for pore water sulfate and AVS for samples from FOAM

Core	Depth (cm)	$\delta^{34}\text{S}$ sulfate (‰)	$\delta^{34}\text{S}$ AVS (‰)	$\delta^{34}\text{S}$ pyrite (‰)
FOAM-1	0	20.5		
FOAM-1	0.5	23.4		-20.1
FOAM-1	1.5	25.1	-18.4	
FOAM-1	2.5	24.7	-21.1	-23.0
FOAM-1	3.5	26.2	-20.3	-23.2
FOAM-1	4.5	25.8	-19.9	-23.4
FOAM-1	5.5	26.8	-20.7	-22.9
FOAM-1	6.5	28.2	-22.7	
FOAM-1	7.5	28.6		-23.1
FOAM-1	10.5	30.9		
FOAM-1	11.5	30.9		
FOAM-1	12.5	32		-23.2
FOAM-1	13.5	33.3		-22.1
FOAM-1	14.5			-21.8
FOAM-1	14.5			-21.7
FOAM-1	15.5	33.8		-21.6
FOAM-1	16.5	33.5		-21.1
FOAM-1	17.5	34.3		
FOAM-1	18.5	34.6		-19.1

The data are presented in figure 4.

$\text{Fe}_{\text{py}}/\text{Fe}_{\text{HR}}$ , and DOP are all similar to those reported or calculated from data published in previous FOAM studies (Krishnaswami and others, 1984; Canfield, 1989; Canfield and others, 1992; Raiswell and Canfield, 1998).

TABLE 2  
Multiple sulfur isotope data from the 2010 FOAM core

Depth	sulfate		sulfide	
	$\delta^{34}\text{S}$ (‰)	$\Delta^{33}\text{S}$ (‰)	$\delta^{34}\text{S}$ (‰)	$\Delta^{33}\text{S}$ (‰)
0 (bw)	20.85	0.040		
2	21.87	0.032		
4	21.44	0.041		
8	23.98	0.036		
12	37.35	0.113	-18.95	0.149
16	36.00	0.104	-19.48	0.155
20	37.97	0.122	-17.80	0.159
24	42.16	0.115	-17.07	0.179
28	43.63	0.117		
32	44.28	0.119		
36	43.65	0.102		
40	43.80	0.116		

The data are presented in figure 4.

TABLE 3  
*Results for Fe speciation, degree of pyritization (DOP), bulk sedimentary Fe and Al concentrations, and total organic carbon (TOC)*

Depth (cm)	Fe <sub>sec</sub> (wt %)	Fe <sub>dit</sub> (wt %)	Fe <sub>mag</sub> (wt %)	Fe <sub>py</sub> (wt %)	Fe <sub>HCl</sub> (wt %)	Fe <sub>T</sub> (wt %)	Al <sub>T</sub> (wt %)	Fe <sub>H2R</sub> /Fe <sub>T</sub>	Fe <sub>py</sub> /Fe <sub>H2R</sub>	Fe <sub>T</sub> /Al	DOP	TOC (wt %)
0.5	0.02	<D.L.	0.09	0.68	1.37	3.18	5.82	0.25	0.86	0.55	0.33	1.75
2	<D.L.	0.11	0.06	0.65	1.14	3.44	6.61	0.24	0.79	0.52	0.36	1.85
4	0.06	0.13	0.05	0.31	1.18	3.16	6.43	0.18	0.55	0.49	0.21	1.20
6	0.03	0.10	0.06	0.36	1.33	2.96	5.67	0.19	0.65	0.52	0.22	1.22
8	0.01	0.04	0.02	0.35	1.05	3.13	6.45	0.14	0.84	0.48	0.25	1.31
10	0.01	0.03	0.02	0.60	0.94	2.72	5.51	0.24	0.91	0.49	0.39	1.01
12	0.01	0.02	0.06	0.66	1.02	2.77	5.71	0.27	0.86	0.48	0.39	2.50
14	<D.L.	<D.L.	0.01	0.74	1.16	3.03	6.03	0.25	0.98	0.50	0.39	1.21
16	0.01	0.02	0.01	0.65	0.94	3.11	6.19	0.22	0.94	0.50	0.41	0.71
18	0.02	0.03	0.03	0.69	1.00	2.53	4.95	0.31	0.89	0.51	0.41	1.04
20	0.05	0.04	0.07	0.71	1.25	3.21	6.04	0.27	0.82	0.53	0.36	1.32
22	<D.L.	<D.L.	0.06	0.93	0.92	3.32	6.67	0.30	0.94	0.50	0.50	1.42
24	0.01	<D.L.	0.05	1.06	1.24	3.12	4.85	0.36	0.95	0.64	0.46	1.52
26	<D.L.	<D.L.	0.07	0.83	1.12	3.69	7.38	0.24	0.93	0.50	0.43	1.65
28	<D.L.	<D.L.	0.04	0.93	1.51	3.45	7.01	0.28	0.96	0.49	0.38	1.24
30	<D.L.	<D.L.	0.02	0.86	0.97	3.03	5.69	0.28	0.99	0.53	0.47	1.45
32	0.04	0.02	0.08	0.68	1.21	3.17	6.12	0.26	0.83	0.52	0.36	1.41
34	0.03	0.01	0.08	0.59	1.24	2.79	5.89	0.26	0.83	0.47	0.32	0.87
36	<D.L.	<D.L.	0.03	0.70	1.10	3.19	6.09	0.23	0.96	0.52	0.39	1.54
38	<D.L.	0.01	0.07	0.69	1.20	3.06	5.87	0.25	0.90	0.52	0.36	1.91
40	0.03	0.03	0.08	0.66	1.17	3.00	5.73	0.27	0.83	0.52	0.36	1.00
42	0.02	0.01	0.06	0.55	1.14	3.28	6.47	0.19	0.87	0.51	0.33	1.47
44	0.02	0.01	0.07	0.71	1.13	3.04	5.70	0.27	0.88	0.53	0.39	1.64
46	0.01	<D.L.	0.09	0.81	0.99	3.31	6.48	0.27	0.89	0.51	0.45	1.49
48	0.02	0.01	0.06	0.60	0.77	3.16	5.84	0.22	0.86	0.54	0.44	1.42
50	<D.L.	<D.L.	0.02	0.85	0.84	2.84	5.22	0.31	0.97	0.54	0.50	1.27

D.L. = Detection limit.  
 The data are presented in figure 5.

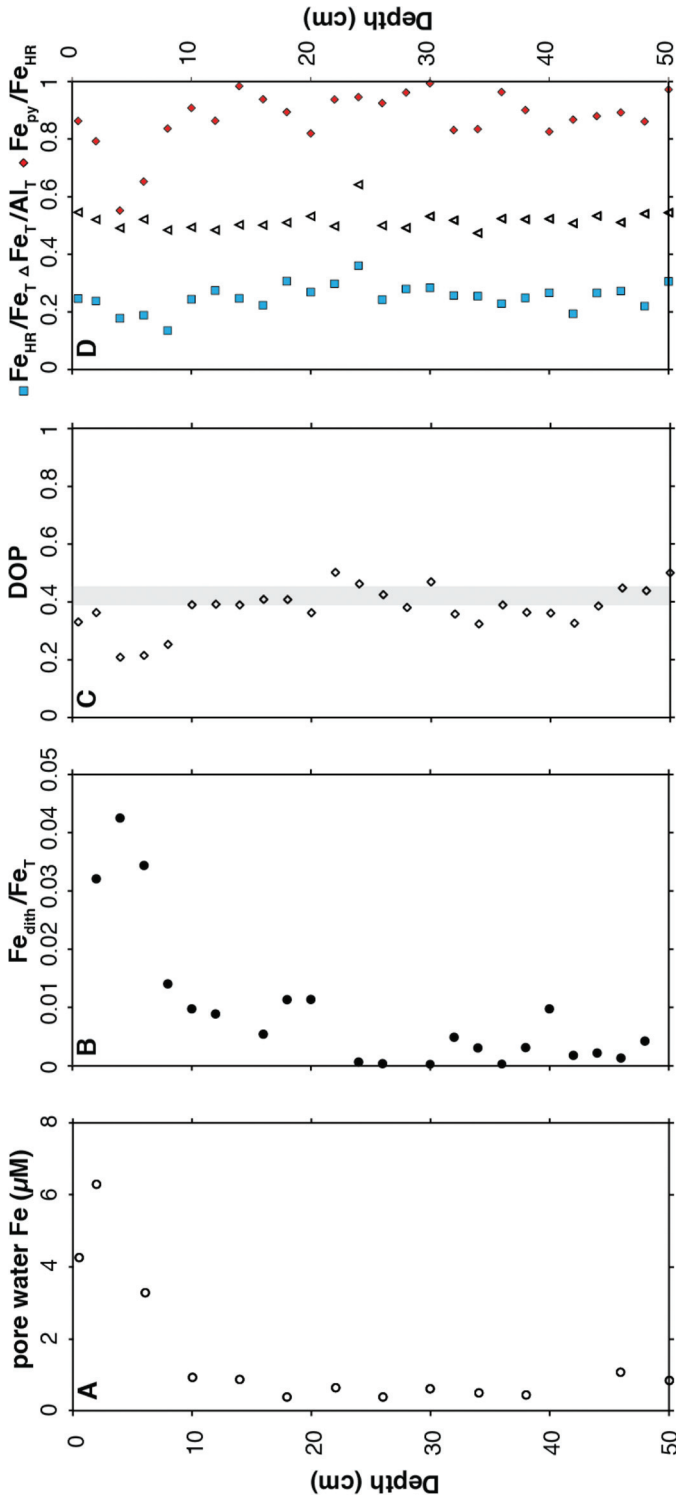


Fig. 5. (A) Dissolved pore water Fe concentrations, (B) dithionite Fe to total Fe ratios ( $\text{Fe}_{\text{dith}}/\text{Fe}_T$ ), (C) degree of pyritization (DOP), and (D) ratios of highly reactive Fe to total Fe concentrations ( $\text{Fe}_{\text{HR}}/\text{Fe}_T$ ), total Fe to Al ratios ( $\Delta\text{Fe}_T/\text{Al}_T$ ), and pyritized Fe over highly reactive Fe ( $\text{Fe}_{\text{py}}/\text{Fe}_{\text{HR}}$ ). The vertical bar represents the range of DOP previously measured at FOAM from Canfield and others (1992).

Solid-phase Mo concentrations at FOAM do not exceed 2 ppm (figs. 6A and 6B; table 4). There is a subsurface pore water Mo maximum of  $\sim 300$  nM at 5 to 7 cm (fig. 6C). Sedimentary Mn concentrations are in the same range as previous work (Aller, 1980b), which also show a homogenous distribution in the upper 10 cm (fig. 6D). The range in pore water Mn (fig. 6E) is similar to that reported for autumn cores in a previous FOAM study (Aller, 1980b). Pore water Mn accumulation overlies the depth of initial sulfide accumulation and overlaps with pore water Mo concentrations elevated above those of seawater (fig. 6).

## DISCUSSION

### *Iron Speciation as a Pore Fluid Paleoredox Indicator*

Iron speciation has been widely used to infer water column paleoredox conditions, but only recently has this application been extended to recognize paleo-pore water sulfide accumulation (Sperling and others, 2015). Applications toward recognizing ancient pore water sulfide accumulation are well grounded in work from modern sites, such as FOAM, but no previous study has evaluated the ability of Fe speciation to uniquely discern pore water sulfide in a diverse range of modern localities. Pore water sulfide does not accumulate until the most 'highly reactive' Fe minerals—for example, ferrihydrite and hematite—are quantitatively titrated in the sediments to form pyrite or other Fe sulfides (Canfield, 1989; Canfield and others, 1992; Raiswell and others, 1994), thus elevated  $\text{Fe}_{\text{py}}/\text{Fe}_{\text{HR}}$  are anticipated for these settings.

In line with expectations, the Fe speciation data compilation in figure 2 provides broad evidence that  $\text{Fe}_{\text{py}}/\text{Fe}_{\text{HR}}$  values are  $<0.7$  in modern sediments where sulfide is independently constrained to be absent. Data from sulfidic pore water systems are less common but, with few exceptions (discussed next paragraph), display  $\text{Fe}_{\text{py}}/\text{Fe}_{\text{HR}}$  ratios  $>0.7$ . Examples of sites with sulfidic pore waters include the FOAM site (this study; Canfield, 1989), Peru Margin (Böning and others, 2004; Scholz and others, 2011), Santa Barbara Basin (Raven and others, 2016), and Argentine Margin (Riedinger and others, 2017). Our FOAM data reveal up to 3 mM of pore water sulfide (fig. 4) and  $\text{Fe}_{\text{py}}/\text{Fe}_{\text{HR}} >0.7$  (fig. 5). Though the collective data from sites without pore water sulfide have  $\text{Fe}_{\text{py}}/\text{Fe}_{\text{HR}} <0.7$ , portions of the FOAM sediment profile without pore water sulfide do have elevated  $\text{Fe}_{\text{py}}/\text{Fe}_{\text{HR}}$  (fig. 5). In the upper 4 cm at FOAM, ratios of  $\text{Fe}_{\text{py}}/\text{Fe}_{\text{HR}}$  and DOP are elevated compared to the remainder of the upper 'sulfide free' zone in part because of dissolution of Fe-oxides to produce dissolved Fe in the pore waters—a 'highly reactive' Fe phase, not included in these proxy calculations. Factors leading to the presence of pyrite in the 'sulfide free' zone may result from sediment mixing, terrigenous input, as well as ongoing sulfate reduction (Canfield and others, 1992; Riedinger and others, 2017). Regardless, the collective data support that paleo-pore water sulfide accumulation can be recognized in the geologic record via  $\text{Fe}_{\text{py}}/\text{Fe}_{\text{HR}}$  values  $>0.7$ ,  $\text{Fe}_{\text{HR}}/\text{Fe}_{\text{T}}$  ratios of  $<0.38$ ,  $\text{DOP} < \sim 0.4$ , and  $\text{Fe}_{\text{T}}/\text{Al} < 0.5$  (Raiswell and others, 1988; Raiswell and Canfield, 1998; Lyons and others, 2003), although threshold values should be applied with caution.

The collective data from sites without stable euxinia suggest that  $\text{Fe}_{\text{py}}/\text{Fe}_{\text{HR}}$  ratios of  $>0.7$  are generally a consistent indicator of pore water sulfide accumulation (fig. 2A), but lower values do not necessarily imply a lack of pore water sulfide. Exceptions include sediments from the Santa Barbara Basin and the Argentine Margin, where pore water sulfide concentrations approach mM levels, yet  $\text{Fe}_{\text{py}}/\text{Fe}_{\text{HR}}$  ratios are  $<0.7$ . The trends in the Argentine Margin are likely a combination of high sedimentation rates and an abundance of magnetite and anomalously high levels of Fe-oxides that react with sulfide to form pyrite (Riedinger and others, 2017). As was shown in a landmark study at the FOAM site, dissolved sulfide reacts with 'reactive' Fe

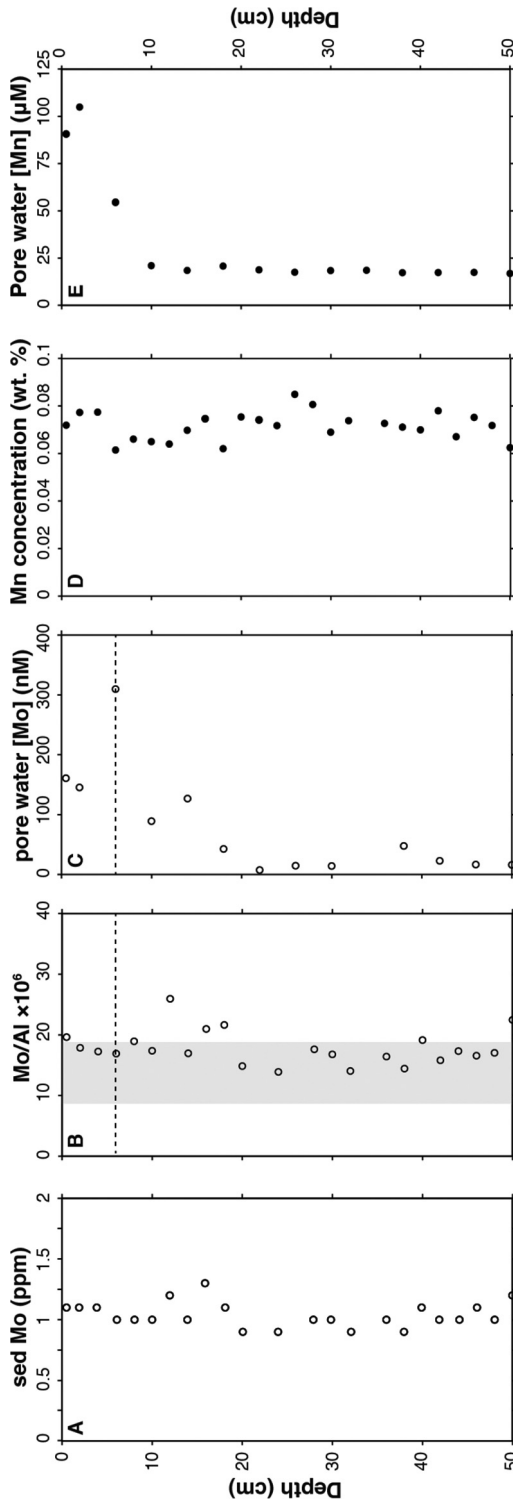


Fig. 6. Sedimentary (A) Mo concentrations, (B) Mo/Al mass ratios, (C) pore water Mo concentrations, (D) sedimentary Mn concentrations, and (E) pore water Mn concentrations. Horizontal dashed lines represent the depth of significant sulfide accumulation. Shaded areas represent Mo/Al average shale values from Turekian and Wedepohl (1961).



TABLE 4  
Sedimentary and pore water Mo concentrations

Depth (cm)	Pore water Mo (nM)	Bulk Mo (ppm)
0.5	157.4	1.1
2	139.8	1.1
4		1.1
6	296.5	1.0
8		1.0
10	79.9	1.0
12		1.2
14	115.1	1.0
16		1.3
18	35.9	1.1
20		0.9
22	3.0	
24		0.9
26	4.5	
28		1.0
30	13.9	1.0
32		0.9
34		
36		1.0
38	34.2	0.9
40		1.1
42	14.4	1.0
44		1.0
46	14.8	1.1
48		1.0
50	8.4	1.2

The data are presented in figure 6.

minerals such as Fe-(oxy)hydroxides and hematite prior to dissolved sulfide accumulation, but the kinetics of the reaction with magnetite are up to seven orders of magnitude slower, thus allowing for pore water sulfide accumulation despite the presence of 'highly reactive' Fe as magnetite (Canfield and others, 1992). Sulfur isotope data at FOAM are consistent with continued pyrite formation from magnetite well below the onset of sulfide accumulation (Canfield and others, 1992). Along the Argentine Margin, sporadic and rapid sedimentation maintain non-steady state geochemical conditions and decrease the residence time of sediments and 'reactive' Fe minerals, including magnetite, in a thin zone of sulfide accumulation (Riedinger and others, 2017). In this zone, the rate of sulfate reduction exceeds reaction rates between dissolved sulfide and the abundance of various 'highly reactive' Fe phases (Riedinger and others, 2017).

To our knowledge, the Fe speciation data compilation in figure 2 is the first to consider both  $Fe_{HR}/Fe_T$  and  $Fe_{py}/Fe_{HR}$  from the full range of modern settings with available data. The original work of Raiswell and Canfield (1998) did not consider  $Fe_{py}/Fe_{HR}$ , but the data compilation presented here generally reinforces their conclusions. Specifically, only sediments from the euxinic Black Sea, Cariaco Basin, and

Framvaren Fjord record clear indications of euxinia from the collective Fe speciation data. Raiswell and Canfield (1998) made the same observation based on their  $Fe_{HR}/Fe_T$  compilation. Other euxinic sites (for example, Orca Basin and Kau Bay) and low oxygen or ‘nitrogenous’ settings with and without intermittent euxinia (for example, Peru Margin) have  $Fe_{HR}/Fe_T < 0.38$  and  $Fe_{py}/Fe_{HR}$  values that are not consistently elevated. Other euxinic settings can fall in this group, particularly when marked by very rapid sedimentation, such as along the Black Sea margin (Lyons and Kashgarian, 2005). For the sample set in figure 2, the only low oxygen (in this case, seasonally anoxic), non-euxinic site to yield  $Fe_{HR}/Fe_T$  ratios of  $> 0.38$  from multiple samples is the Santa Barbara Basin (Raven and others, 2016), where the Fe speciation data are in a range typically interpreted as reflective of ferruginous conditions. Redox boundaries, either temporal or spatial, have been suggested as necessary for elevated Fe-oxide delivery relative to detrital values, and thus Fe speciation indications of ferruginous conditions (Scholz and others, 2014a; Scholz and others, 2014b; Hardisty and others, 2016), but such settings are seemingly rare in the modern ocean. It is possible, however, that Fe speciation evidence for ferruginous conditions may be more common than currently known in sediments from modern low oxygen settings lacking persistent water column sulfide accumulation. To date, each of the modern low oxygen or euxinic localities measured for Fe speciation only include  $Fe_{py}$  and  $Fe_{dith}$  as part of the ‘highly reactive’ Fe pool (Raiswell and Canfield, 1998; Scholz and others, 2014b; Raven and others, 2016). Consideration of  $Fe_{HR}/Fe_T$  and  $Fe_{py}/Fe_{HR}$  without  $Fe_{mag}$  and  $Fe_{carb}$  specifically makes ferruginous settings more difficult to identify (Raiswell and others, 2018).

Lastly, some oxic localities—specifically nearshore deltaic and fjordic sites characterized by rapid sediment reworking and high  $Fe_{HR}/Fe_T$  in the source sediments—yield Fe speciation values also consistent with ferruginous conditions (Poulton and Raiswell, 2002; Aller and others, 2004; März and others, 2012). Similar trends can be found in  $Fe_T/Al$  for some of these localities, with mass ratios exceeding the  $\sim 0.5$  typical of sediments underlying oxic waters. Such observations stress the necessity to consider local  $Fe_{HR}/Fe_T$  and  $Fe_T/Al$  detrital baselines, the sedimentary context, and independent paleoredox proxies when interpreting Fe geochemistry from ancient settings (Cole and others, 2017; Raiswell and others, 2018).

#### *Molybdenum Concentrations as a Pore Fluid Paleoredox Indicator*

Concentrations of Mo and Fe speciation are commonly used to infer the presence of ancient water column sulfide and some recent studies provide evidence that unique ranges exist for Mo concentrations beneath modern non-euxinic water columns containing pore water sulfide (Scott and Lyons, 2012). Our compilation of Mo concentrations from oxic settings with and without pore water sulfide support these applications and past studies (fig. 3). Specifically, sedimentary Mo concentrations above crustal values but  $< 40$  ppm—but mostly  $< 10$  ppm—and with independent constraints of oxic water column conditions can generally be attributed to the presence of pore water sulfide (fig. 3A). The authigenic Mo enrichments in oxic settings with sulfidic pore fluids is largely a function of a Mn or Fe oxide shuttle that delivers Mo to the sediments, and then fixation with sulfide following reductive dissolution of the oxides (Zheng and others, 2000; Scott and Lyons, 2012). Indeed, the range in Mo concentrations from oxic settings with sulfidic pore fluids is largely derived from settings with a clear enrichment in Mn and Mo at the surface (omitted from compilation in fig. 3) and a secondary enrichment in Mo following a decrease in Mn concentrations below the zone of sulfide accumulation (Scott and Lyons, 2012). For example, this relationship is observed from sediment at Loch Etive, Scotland (Malcolm, 1985), and an estuary in British Columbia (Pedersen, 1985). These observations can be clearly contrasted by environments with surficial Mn enrichments that lack

an adjacent subsurface zone of sulfide accumulation, such as some hemipelagic sediments (Shimmield and Price, 1986). In hemipelagic sediments, large Mo enrichments—in some cases 100s of ppm—can occur in Mn,Fe-crusts in the upper sediment zone, but decrease to near-detrital values upon Mn and Fe dissolution, and thus elevated concentrations are not preserved in the geologic record.

Importantly, we acknowledge that Mo concentrations from low oxygen settings with intermittent water column and pore water sulfide have concentrations similar to many stable euxinic settings and oxic settings with pore water sulfide (fig. 3B). This is important for the proxy perspective presented here, as the current  $Fe_{HR}/Fe_T$  data from low oxygen and intermittently euxinic localities overlap with that of oxic settings (fig. 2), indicating a need for further proxies for distinction. Additional redox proxies which can discriminate low oxygen settings from oxic settings include U concentrations (Sundby and others, 2004; McManus and others, 2006; Algeo and Tribovillard, 2009; Scholz and others, 2011), Mo isotopes (Poulson Brucker and others, 2009; Hardisty and others, 2016; Scholz and others, 2017), nitrogen isotopes (Scholz and others, 2017), and iodine contents (Owens and others, 2017; Zhou and others, 2017). In addition, a relationship between TOC and Mo concentrations like that from the Peruvian (Böning and others, 2004; Scholz and others, 2011; Scholz and others, 2017) and Namibian (Calvert and Price, 1983; Algeo and Lyons, 2006) oxygen minimum zones (OMZs) is not observed in oxic settings (Algeo and Lyons, 2006).

One possible explanation of the elevated Mo concentrations in these mostly ‘nitrogenous’ localities is the intermittent accumulation of low water column hydrogen sulfide; however, thermodynamic considerations and observations from weakly sulfidic plumes ( $<15 \mu\text{M}$ ) in the Peru OMZ have been suggested as inconsistent with Mo scavenging in these waters (Scholz and others, 2016; Scholz and others, 2017). We point out that multiple field and theoretical studies indicate a requirement of significant dissolved sulfide accumulation ( $>100 \mu\text{M}$ ) prior to authigenic Mo accumulation (Helz and others, 1996; Erickson and Helz, 2000; Zheng and others, 2000; Helz and others, 2011; Helz and others, 2011; Chappaz and others, 2014; Dahl and others, 2017; Wagner and others, 2017). In addition, a distinct relationship between Mo and TOC, like that observed in the Peruvian (Böning and others, 2004; Scholz and others, 2011; Scholz and others, 2017) and Namibian (Calvert and Price, 1983; Algeo and Lyons, 2006) upwelling zones, is otherwise uniquely attributed to settings with at least intermittent water column sulfide accumulation (Algeo and Lyons, 2006). Additional mechanisms of authigenic Mo enrichments from low oxygen localities include sedimentary delivery via oxides during episodic bottom water oxygenation and Mo fixation following reaction with pore water sulfide (Algeo and Tribovillard, 2009; Scholz and others, 2011; Scholz and others, 2017). In our data compilation, Mo concentrations from low oxygen settings with and without pore water sulfide present during sampling are not distinguishable (fig. 3C). This observation likely stems from intermittent or past pore water and water column sulfide accumulation not captured or recognized during sampling.

Lastly, even with elevated pore water sulfide concentrations, a number of factors in oxic localities can lead to a lack of Mo enrichments beyond detrital values. This is evident from figure 3, which shows that there is an overlap in the Mo concentration range from oxic settings with and without pore water sulfide accumulation. In the next section, we provide a case study from the FOAM site, where we observe elevated pore water sulfide, but sedimentary Mo concentrations are near detrital values. Ultimately, oxic settings with and without pore water sulfide accumulation can be discerned via  $Fe_{py}/Fe_{HR}$  values (fig. 2). However, as discussed below, the lack of authigenic Mo enrichments from sediments with  $Fe_{py}/Fe_{HR} > 0.8$  may provide additional insights to early diagenetic processes in ancient settings, including sedimentation rates and

seasonal oxidative processes. A diagenetic model is used to demonstrate the conditions leading to the range of authigenic Mo enrichments observed in figure 3.

#### FOAM Case Study and Diagenetic Model

Previous studies have not measured Mo at FOAM, but localities with water column redox and diagenetic regimes similar to FOAM, such as an adjacent site in New Haven Harbor and Boston Harbor, Massachusetts, USA, have reported sedimentary Mo enrichments up to 8 ppm (Bertine and Turekian, 1973; Morford and others, 2007). These Mo concentrations are easily distinguished from detrital values (1–2 ppm) and are well below Mo concentrations typical of sediments underlying euxinic water columns (Scott and Lyons, 2012). The up to 3 mM sulfide levels at FOAM are well above the 100  $\mu\text{M}$  ‘action point’ for total dissolved sulfide concentration that favors the transformation of molybdate to tetrathiomolybdate, which can then be efficiently, often quantitatively, scavenged (Helz and others, 1996; Zheng and others, 2000). In sulfidic sediments, following Mn and Fe oxide dissolution, near-complete authigenic Mo removal from pore waters typically occurs at the transition zone to sulfide accumulation, forming a deeper second solid-phase Mo peak (Scott and Lyons, 2012). Sedimentary Mo peaks are not observed at all at FOAM despite pore water Mo levels greater than those of the overlying seawater and a clear indication of subsurface Mn and Fe oxide reduction seen in both pore water and sediment data (figs. 5 and 6). Below we consider sediment mass balance and a diagenetic model for Mo to determine the factors that influence authigenic Mo enrichments at FOAM and other non-euxinic localities.

We use estimates of the lithogenic Mo ( $\text{Mo}_{\text{lith}}$ ) input relative to the observed bulk Mo concentrations ( $\text{Mo}_{\text{bulk}}$ ) to determine the contribution, if any, from authigenic Mo ( $\text{Mo}_{\text{auth}}$ ):

$$\text{Mo}_{\text{bulk}} = \text{Mo}_{\text{lith}} + \text{Mo}_{\text{auth}} \quad (3)$$

Although constraints on the lithogenic input of Mo to sediments in Long Island Sound are lacking, we can estimate this component using a bulk average value of Mo/Al for granite- and sandstone-derived lithogenic material of  $8\text{--}18 \times 10^{-6}$  (Turekian and Wedepohl, 1961; McLennan, 2001; Poulson Brucker and others, 2009). Both rock types are common regionally near FOAM. This lithogenic Mo range also overlaps with baseline Mo concentrations found in Buzzards Bay and Boston Harbor, Massachusetts (Morford and others, 2007; Morford and others, 2009), which have similar weathering source rocks. Considering an average sedimentary Al concentration of 6.0 weight percent at FOAM (table 3), we calculate a lithogenic Mo input of 0.36 to 1.4 ppm. This contribution is negligible for sediments with large authigenic Mo enrichments, but considering an average Mo concentration for FOAM sediments of 1.02 ppm,  $\text{Mo}_{\text{lith}}$  has the potential to make up anywhere from 35 to 100 percent of the bulk Mo concentrations. If authigenic Mo is accumulating at FOAM, it is clearly at very low concentrations.

The total authigenic consumption flux of dissolved Mo within marine sediments can be quantitatively estimated using an early diagenetic model (eq. 4). The model tracks solid (organic matter accumulation and authigenic tetrathiomolybdate formation) and dissolved phases (Mo,  $\text{H}_2\text{S}$ ,  $\text{O}_2$ ) in diffusional exchange with seawater, within the upper 200 cm of the sediment column.

$$\frac{\partial[\text{X}]}{\partial t} = D \frac{\partial^2[\text{X}]}{\partial z^2} - \omega \frac{\partial[\text{X}]}{\partial z} - \text{rxn} \quad (4)$$

Parameters and associated citations are given in table 5. The sum reaction of the time rate of change of dissolved species in pore waters can be described as the sum of

TABLE 5

*Variables and values used for model calibration and sensitivity tests in figure 7*

Parameters	Values	Units	Sources
Dissolved seawater [Mo]	150	nM	(this study – FOAM)
Dissolved seawater [O <sub>2</sub> ]	150	μM	
Mo Diffusion coefficient ( $D_{Mo}$ )	391	cm <sup>2</sup> yr <sup>-1</sup>	(Malinovsky and others, 2007)
O <sub>2</sub> Diffusion coefficient ( $D_{O_2}$ )	621	cm <sup>2</sup> yr <sup>-1</sup>	(Ferrell and Himmelblau, 1967; Hayduk and Laudie, 1974)
Sedimentation rate ( $\omega$ )	0.2	cm yr <sup>-1</sup>	(Goldhaber and others, 1977; Krishnaswami and others, 1984)
Sediment porosity ( $\phi$ )	0.8	-	(Boudreau, 1997)
Organic rate constant ( $k_{org}$ )	$4.0 \times 10^{-3}$	yr <sup>-1</sup>	(Arndt and others, 2009) (this study – FOAM)
Thiomolybdate rate constant ( $k_{th}$ )	$1 \times 10^3$	mmol cm <sup>-2</sup> yr <sup>-1</sup>	(this study – FOAM)
Limiting concentration for O <sub>2</sub> ( $K_{O_2}$ )	$20 \times 10^{-6}$	mmol cm <sup>-3</sup>	(Reed and others, 2011)
Organic rain flux ( $F_{org}$ )	0.3	mmol cm <sup>-2</sup> yr <sup>-1</sup>	(this study – FOAM)

the diffusion term ( $D \frac{\partial^2 [X]}{\partial z^2}$ ), the advection term ( $\omega \frac{\partial [X]}{\partial z}$ ), and the reaction term (rxn). The variable  $D$  is the diffusion coefficient,  $\omega$  is the sedimentation rate, and  $z$  the depth away from the sediment-water interface (Boudreau, 1997). The consumption of oxygen through aerobic respiration of organic matter was parameterized as  $k_{org} [org] \frac{[O_2]}{[O_2] + k_{O_2}}$ , where  $k_{org}$  is the reaction rate constant and  $k_{O_2}$  the limiting concentration for O<sub>2</sub>. The term  $\frac{\partial [Mo]}{\partial z}$  considers the gradient in pore water Mo concentrations from the depth of O<sub>2</sub> consumption—and hence the onset of oxide dissolution and associated release of sorbed Mo—to the depth where Mo concentrations decrease to stable values within the zone of pore water sulfide accumulation. The reaction term for tetrathiomolybdate is expressed as  $k_{th} [H_2S] [Mo]$ , where  $k_{th}$  is the reaction rate constant. The  $k_{org}$  and  $k_{th}$  were determined by calibrating the model to pore water Mo and sulfide data derived from the FOAM site (table 5). Dissolved sulfide levels were set at a constant value under conditions where oxygen has been quantitatively consumed through respiration. Further, if [O<sub>2</sub>] is greater than zero, [H<sub>2</sub>S] is assumed to be zero.

Next, we explore the sensitivity of authigenic Mo enrichments within marine sediments over a wide range of parameter space considered in figure 3 and the associated discussions—but using FOAM site values as a baseline (fig. 7; table 5). At the most basic level, the delivery of organic carbon and the associated accumulation of pore water sulfide through sulfate reduction is a requirement from the model in order to achieve even muted authigenic Mo enrichments (figs. 7D and 7E). The model is sensitive to pore water Mo concentrations at the depth of O<sub>2</sub> consumption (fig. 7A), which implies that higher delivery of Mo to the sediments via oxides and burial and diffusion of seawater will increase authigenic enrichments upon reaction of the

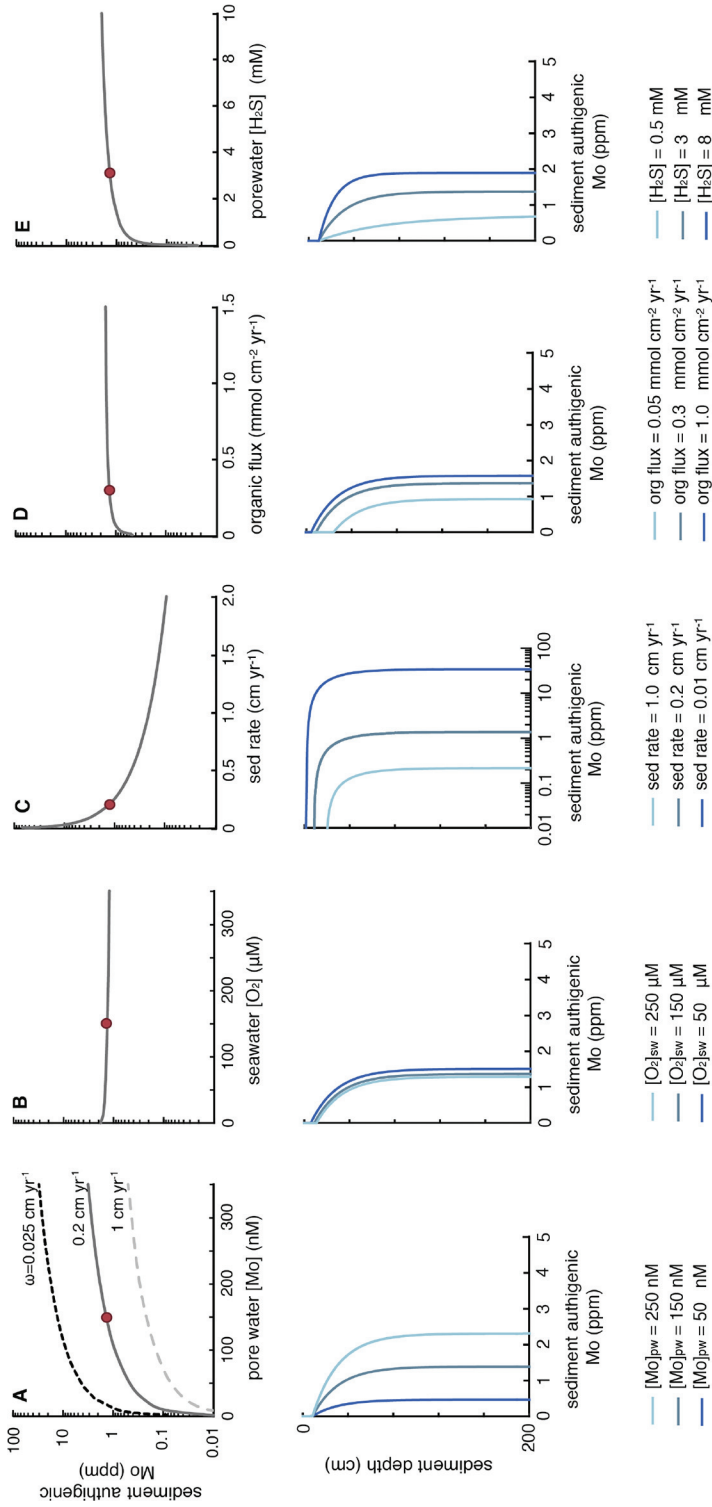


Fig. 7. Diagenetic model results. Baseline values (red dot) are parameters determined from the FOAM site and are presented in table 5. Unless otherwise indicated, the model sensitivity analyses use the FOAM values for relevant parameters. We explore the sensitivity of marine authigenic Mo enrichments to dissolved seawater Mo and O<sub>2</sub>, sedimentation rates, organic matter rain flux and porewater H<sub>2</sub>S levels over a wide range of parameter space relevant to that considered in figure 3.

dissolved Mo with appreciable pore water sulfide. As in similar previous models (Morford and others, 2009), we find authigenic Mo enrichment to be most highly sensitive to sedimentation rates (figs. 7A and 7C). For example, sedimentation of  $>0.2$   $\text{cm yr}^{-1}$  can severely mute authigenic enrichments in marginal settings such as FOAM, explaining the observed sediment Mo concentration values (fig. 6). Muted Mo concentrations have even been observed from euxinic portions of the Black Sea where sedimentation rates are elevated (Lyons and Kashgarian, 2005). Conversely, particularly low sedimentation rates in combination with elevated pore water Mo at the depth of  $\text{O}_2$  consumption can allow for relatively elevated authigenic Mo concentrations (figs. 7A and 7C). These conditions replicate the ranges of Mo concentrations observed from other oxic sites with pore water sulfide and elevated authigenic enrichments (fig. 3). In addition, if we consider a sensitivity analysis that integrates the most extreme  $\frac{\partial[\text{Mo}]}{\partial z}$  and  $\omega$  from Peru Margin Sites with available data ( $\sim 350$  nM and  $\sim 0.025$   $\text{cm yr}^{-1}$ , respectively; Scholz and others, 2011), the model provides evidence that sedimentary Mo concentration of up to  $\sim 70$  ppm are possible (figs. 7A and 7C)—a range which explains the bulk of the existing sedimentary Mo data from low oxygen environments (fig. 3). However, under no relevant conditions can the model replicate the  $>100$  ppm Mo found in some of these low oxygen environments (Brongersma-Sanders and others, 1980; Calvert and Price, 1983; Böning and others, 2004; Scholz and others, 2011; Scholz and others, 2017). Such a result provides evidence that water column sulfide accumulation, or additional sedimentary Mo delivery parameters not considered in our model are likely necessary to explain the extreme elevated Mo enrichments from these low oxygen settings (fig. 3; Scholz and others, 2017).

Lastly, though sedimentation rates and sedimentary Mo delivery can explain the ranges of authigenic Mo accumulation from oxic settings, seasonal variations in sediment chemistry not considered in our model are all likely to contribute to muted authigenic Mo formation. Previous studies have shown that sediments with seasonal variations in redox state, metabolic rates, or biogenic mixing of particles between redox zones of the sediments, like FOAM (Goldhaber and others, 1977; Aller, 1980a, 1980b), minimize retention of authigenic Mo phases (Morford and others, 2009; Wang and others, 2011). At FOAM, a range of previous work provides evidence that bioturbation, pore water redox, and organic matter remineralization rates all vary seasonally within the upper few cm of the sediment pile (Goldhaber and others, 1977; Aller, 1980a, 1980b). Specifically, lower temperatures during the winter months decrease infaunal activity and metabolic rates. Together, these processes result in relatively more oxidizing conditions near the sediment water interface during the winter relative to summer through decreased upward mixing of reduced sediments and decreased rates of sulfate reduction, with the consequence of net oxidation of reduced sedimentary phases such as pyrite (Goldhaber and others, 1977; Aller, 1980a, 1980b; Westrich and Berner, 1988; Green and Aller, 1998, 2001). However, despite these known dynamics, data generated for this study that overlap with that of previous FOAM works [S isotopes (fig. 4D); dissolved Fe and Mn, and sulfide; sedimentary Fe speciation, Mn, and S concentrations] are remarkably comparable despite, in some cases, nearly 40 years difference in the time of our sampling (see Results section for details). Indeed, despite temperature, metabolic, and faunal seasonal dynamics which induce non-steady state sedimentary and geochemical conditions in the upper  $\sim 10$  cm, previous seasonal observations have also proven a consistency of dissolved and sedimentary geochemical characteristics for a given season from year to year (Aller, 1980a, 1980b). Non-steady state factors should be considered in future models, but previous studies and ours provide evidence that FOAM may be best characterized as a 'dynamic steady state.'

## CONCLUSIONS

Based on observations from modern settings, we provide constraints on the use of sedimentary Fe speciation and Mo concentrations as paleoredox proxies to uniquely identify the presence/absence of pore water sulfide accumulation during early diagenesis in ancient non-euxinic water column settings. To this end, we compare ratios of pyrite-to-'highly reactive' Fe ( $Fe_{py}/Fe_{HR}$ ) and Mo concentrations from modern non-euxinic settings with and without observations of sedimentary pore water sulfide accumulation. We also provide original Fe speciation, sedimentary Mo, and S isotope data from the FOAM site in Long Island Sound, where pore water sulfide concentrations are in excess of 3 mM. The FOAM site has played an essential role in our understanding of Fe reactivity toward sulfide and the development of a commonly applied Fe speciation scheme (Canfield and Berner, 1987; Berner and Canfield, 1989; Canfield and others, 1992; Raiswell and Canfield, 1998) and the earlier DOP approach (Berner, 1970; Raiswell and others, 1988; Canfield and others, 1992)—in large part through proximity to Yale University and the research group of Bob Berner. Given previous observations at FOAM and other similar localities with pore water sulfide, we expected  $Fe_{HR}/Fe_T$  values of  $<0.38$  (Raiswell and Canfield, 1998),  $Fe_T/Al$  ratios of  $\sim 0.5$ , (Krishnaswami and others, 1984),  $Fe_{py}/Fe_{HR} > 0.8$ , and Mo concentrations 2 to 25 ppm (Scott and Lyons, 2012). Deviations from these predictions are explored in the context of the broader data compilation and sensitivity analyses of an authigenic Mo model.

Iron speciation data from the literature and our new FOAM results fit the predicted ranges, with most of the 'highly reactive' Fe pool reacted with  $\Sigma H_2S$  to form pyrite and resulting, with few exceptions, in  $Fe_{py}/Fe_{HR}$  values as a generally confident indicator of the presence/absence of pore water sulfide accumulation during early diagenesis. Molybdenum concentrations at FOAM, by contrast, did not fall within the typical range for sulfidic pore fluids (Scott and Lyons, 2012). Oxic settings with pore water sulfide accumulation, including FOAM, commonly display Mo concentrations similar to detrital values, hence overlapping with that observed in oxic settings lacking pore water sulfide. A diagenetic model that considers pore water dissolved Mo, bottom water  $O_2$ , pore water sulfide, sedimentation rate, and organic rain rates provides evidence that there is indeed an authigenic Mo flux to the sediments at FOAM, but that episodic and generally high sedimentation rates likely prevent expression beyond typical lithologic values. In addition, low oxygen (but non-euxinic) water column environments—most prominently the Peru Margin—have the potential for a large range of Mo concentrations, regardless of pore water redox, overlapping with both euxinic settings and oxic environments with pore water sulfide. The additional application of Fe speciation differentiates euxinic and low oxygen (non-euxinic) settings, but other paleoredox proxies (for example, U concentrations, N isotopes, Mo isotopes, iodine contents) are necessary to discern low oxygen environments from oxic settings. If paleoredox indicators beyond Fe speciation and Mo concentrations provide independent constraints on oxic water column conditions, Mo concentrations are a generally reliable indicator of pore water sulfide accumulation.

Overall, our results confirm that Fe speciation applications to identify ancient pore water sulfide accumulation are reasonable, similar to applications of Sperling and others (2015), but point to the requirement of more nuanced considerations for similar applications of Mo concentrations. When Fe speciation and Mo concentrations are applied together to ancient sediments, the modern framework and authigenic Mo model combined here may be used to constrain trends in pore water sulfide accumulation and modes and ranges of Mo delivery to non-euxinic sediments. These constraints provide a context for tracking evolutionary trends in benthic habitation as well as controls on seawater sulfate and Mo concentrations through time.



## ACKNOWLEDGMENTS

An iron-sulfur study of the FOAM site requires acknowledgment and gratitude for the decades of preceding work at the site fundamental to our understanding of early diagenesis and commonly applied paleo proxies. We note, first and foremost, the pioneering work of the late Bob Berner. His contributions, as well as his explicit and implicit anticipation of all the important next steps in iron biogeochemistry, made this study possible. We dedicate this paper to his memory with respect, admiration, and gratitude. Others, Don Canfield and Rob Raiswell in particular, are no less deserving of acknowledgment and gratitude.

DSH, TWL, NJP, and CTR acknowledge support from the NASA Astrobiology Institute under Cooperative Agreement No. NNA15BB03A issued through the Science Mission Directorate. Financial support was provided to NR and TWL by NSF-OCE and an appointment to the NASA Postdoctoral Program, as well as to BCG via a postdoctoral fellowship from the Agouron Institute. DSH was supported by a WHOI postdoctoral fellowship. This manuscript benefited considerably from reviews from Jack Middleburg and one anonymous reviewer.

## REFERENCES

- Algeo, T. J., and Lyons, T. W., 2006, Mo–total organic carbon covariation in modern anoxic marine environments: Implications for analysis of paleoredox and paleohydrographic conditions: *Paleoceanography and Paleoclimatology*, v. 21, n. 1, <https://doi.org/10.1029/2004PA001112>
- Algeo, T. J., and Tribouillard, N., 2009, Environmental analysis of paleoceanographic systems based on molybdenum–uranium covariation: *Chemical Geology*, v. 268, n. 3–4, p. 211–225, <https://doi.org/10.1016/j.chemgeo.2009.09.001>
- Aller, R. C., 1980a, Diagenetic processes near the sediment-water interface of Long Island sound. I.: Decomposition and nutrient element geochemistry (S, N, P): *Advances in Geophysics*, v. 22, p. 237–350, [https://doi.org/10.1016/S0065-2687\(08\)60067-9](https://doi.org/10.1016/S0065-2687(08)60067-9)
- 1980b, Diagenetic processes near the sediment-water interface of Long Island Sound. II. Fe and Mn: *Advances in Geophysics*, v. 22, p. 351–415, [https://doi.org/10.1016/S0065-2687\(08\)60068-0](https://doi.org/10.1016/S0065-2687(08)60068-0)
- Aller, R. C., and Cochran, J. K., 1976,  $^{234}\text{Th}/^{238}\text{U}$  disequilibrium in near-shore sediment: Particle reworking and diagenetic time scales: *Earth and Planetary Science Letters*, v. 29, n. 1, p. 37–50, [https://doi.org/10.1016/0012-821X\(76\)90024-8](https://doi.org/10.1016/0012-821X(76)90024-8)
- Aller, R. C., Hannides, A., Heilbrun, C., and Panzeca, C., 2004, Coupling of early diagenetic processes and sedimentary dynamics in tropical shelf environments: The Gulf of Papua deltaic complex: *Continental Shelf Research*, v. 24, n. 19, p. 2455–2486, <https://doi.org/10.1016/j.csr.2004.07.018>
- Anderson, T. F., and Raiswell, R., 2004, Sources and mechanisms for the enrichment of highly reactive iron in euxinic Black Sea sediments: *American Journal of Science*, v. 304, n. 3, p. 203–233, <https://doi.org/10.2475/ajs.304.3.203>
- Aquilina, A., Homoky, W. B., Hawkes, J. A., Lyons, T. W., and Mills, R. A., 2014, Hydrothermal sediments are a source of water column Fe and Mn in the Bransfield Strait, Antarctica: *Geochimica et Cosmochimica Acta*, v. 137, p. 64–80, <https://doi.org/10.1016/j.gca.2014.04.003>
- Arndt, S., Hetzel, A., and Brumsack, H.-J., 2009, Evolution of organic matter degradation in Cretaceous black shales inferred from authigenic barite: A reaction-transport model: *Geochimica et Cosmochimica Acta*, v. 73, n. 7, p. 2000–2022, <https://doi.org/10.1016/j.gca.2009.01.018>
- Barling, J., and Anbar, A. D., 2004, Molybdenum isotope fractionation during adsorption by manganese oxides: *Earth and Planetary Science Letters*, v. 217, n. 3–4, p. 315–329, [https://doi.org/10.1016/S0012-821X\(03\)00608-3](https://doi.org/10.1016/S0012-821X(03)00608-3)
- Benninger, L., Aller, R., Cochran, J., and Turekian, K., 1979, Effects of biological sediment mixing on the  $^{210}\text{Pb}$  chronology and trace metal distribution in a Long Island Sound sediment core: *Earth and Planetary Science Letters*, v. 43, n. 2, p. 241–259, [https://doi.org/10.1016/0012-821X\(79\)90208-5](https://doi.org/10.1016/0012-821X(79)90208-5)
- Benoit, G. J., Turekian, K. K., and Benninger, L. K., 1979, Radiocarbon dating of a core from Long Island Sound: *Estuarine and Coastal Marine Science*, v. 9, n. 2, p. 171–180, [https://doi.org/10.1016/0302-3524\(79\)90112-9](https://doi.org/10.1016/0302-3524(79)90112-9)
- Berner, R. A., 1970, Sedimentary pyrite formation: *American Journal of Science*, v. 268, n. 1, p. 1–23, <https://doi.org/10.2475/ajs.268.1.1>
- Berner, R. A., and Canfield, D. E., 1989, A new model for atmospheric oxygen over Phanerozoic time: *American Journal of Science*, v. 289, n. 4, p. 333–361, <https://doi.org/10.2475/ajs.289.4.333>
- Berner, R. A., and Westrich, J. T., 1985, Bioturbation and the early diagenesis of carbon and sulfur: *American Journal of Science*, v. 285, n. 3, p. 193–206, <https://doi.org/10.2475/ajs.285.3.193>
- Bertine, K. K., and Turekian, K. K., 1973, Molybdenum in marine deposits: *Geochimica et Cosmochimica Acta*, v. 37, n. 6, p. 1415–1434, [https://doi.org/10.1016/0016-7037\(73\)90080-X](https://doi.org/10.1016/0016-7037(73)90080-X)
- Böning, P., Brumsack, H.-J., Böttcher, M. E., Schnetger, B., Kriete, C., Kallmeyer, J., and Borchers, S. L., 2004, Geochemistry of Peruvian near-surface sediments: *Geochimica et Cosmochimica Acta*, v. 68, n. 21, p. 4429–4451, <https://doi.org/10.1016/j.gca.2004.04.027>

- Boudreau, B. P., 1997, Diagenetic models and their implementation: Berlin, Springer, 430 p.
- Boudreau, B. P., and Canfield, D. E., 1988, A provisional diagenetic model for pH in anoxic porewaters: Application to the FOAM site: *Journal of Marine Research*, v. 46, n. 2, p. 429–455, <https://doi.org/10.1357/002224088785113603>
- Broecker, W. S., and Peng, T.-H., 1982, *Tracers in the Sea*: Palisades, New York, Lamont Doherty Geological Observatory, Eldigio Press, 690 p.
- Brongersma-Sanders, M., Stephan, K., Kwee, T. G., and De Bruin, M., 1980, Distribution of minor elements in cores from the Southwest Africa shelf with notes on plankton and fish mortality: *Marine Geology*, v. 37, n. 1–2, p. 91–132, [https://doi.org/10.1016/0025-3227\(80\)90013-4](https://doi.org/10.1016/0025-3227(80)90013-4)
- Calvert, S. E., and Price, N. B., 1983, Geochemistry of Namibian shelf sediments, in Suess, E., and Thiede, J., editors, *Coastal Upwelling Its Sediment Record*: NATO Conference Series, v. 108, p. 337–375, [https://doi.org/10.1007/978-1-4615-6651-9\\_17](https://doi.org/10.1007/978-1-4615-6651-9_17)
- Canfield, D. E., 1989, Reactive iron in marine sediments: *Geochimica et Cosmochimica Acta*, v. 53, n. 3, p. 619–632, [https://doi.org/10.1016/0016-7037\(89\)90005-7](https://doi.org/10.1016/0016-7037(89)90005-7)
- Canfield, D. E., and Berner, R. A., 1987, Dissolution and pyritization of magnetite in anoxic marine sediments: *Geochimica et Cosmochimica Acta*, v. 51, n. 3, p. 645–659, [https://doi.org/10.1016/0016-7037\(87\)90076-7](https://doi.org/10.1016/0016-7037(87)90076-7)
- Canfield, D. E., and Farquhar, J., 2009, Animal evolution, bioturbation, and the sulfate concentration of the oceans: *Proceedings of the National Academy of Sciences of the United States of America*, v. 106, n. 20, p. 8123–8127, <https://doi.org/10.1073/pnas.0902037106>
- Canfield, D. E., and Thamdrup, B., 1994, The production of  $^{34}\text{S}$ -depleted sulfide during bacterial disproportionation of elemental sulfur: *Science*, v. 266, n. 5193, p. 1973–1975, <https://doi.org/10.1126/science.11540246>
- Canfield, D. E., Raiswell, R., Westrich, J. T., Reaves, C. M., and Berner, R. A., 1986, The use of chromium reduction in the analysis of reduced inorganic sulfur in sediments and shales: *Chemical Geology*, v. 54, n. 1–2, p. 149–155, [https://doi.org/10.1016/0009-2541\(86\)90078-1](https://doi.org/10.1016/0009-2541(86)90078-1)
- Canfield, D. E., Raiswell, R., and Bottrell, S. H., 1992, The reactivity of sedimentary iron minerals toward sulfide: *American Journal of Science*, v. 292, n. 9, p. 659–683, <https://doi.org/10.2475/ajs.292.9.659>
- Canfield, D. E., Lyons, T. W., and Raiswell, R., 1996, A model for iron deposition to euxinic Black Sea sediments: *American Journal of Science*, v. 296, n. 7, p. 818–834, <https://doi.org/10.2475/ajs.296.7.818>
- Canfield, D. E., Poulton, S. W. and Narbonne, G. M., 2007, Late-Neoproterozoic deep-ocean oxygenation and the rise of animal life: *Science*, v. 315, n. 5808, p. 92–95, <https://doi.org/10.1126/science.1135013>
- Chappaz, A., Lyons, T. W., Gregory, D. D., Reinhard, C. T., Gill, B. C., Li, C., and Large, R. R., 2014, Does pyrite act as an important host for molybdenum in modern and ancient euxinic sediments?: *Geochimica et Cosmochimica Acta*, v. 126, p. 112–122, <https://doi.org/10.1016/j.gca.2013.10.028>
- Cline, J. D., 1969, Spectrophotometric determination of hydrogen sulfide in natural waters: *Limnology and Oceanography*, v. 14, n. 3, p. 454–458, <https://doi.org/10.4319/lo.1969.14.3.0454>
- Cole, D. B., Zhang, S., and Planavsky, N. J., 2017, A new estimate of detrital redox-sensitive metal concentrations and variability in fluxes to marine sediments: *Geochimica et Cosmochimica Acta*, v. 215, p. 337–353, <https://doi.org/10.1016/j.gca.2017.08.004>
- Dahl, T., Chappaz, A., Hoek, J., McKenzie, C. J., Svane, S. and Canfield, D., 2017, Evidence of molybdenum association with particulate organic matter under sulfidic conditions: *Geobiology*, v. 15, n. 2, p. 311–323, <https://doi.org/10.1111/gbi.12220>
- Emerson, S. R., and Husted, S. S., 1991, Ocean anoxia and the concentrations of molybdenum and vanadium in seawater: *Marine Chemistry*, v. 34, n. 3–4, p. 177–196, [https://doi.org/10.1016/0304-4203\(91\)90002-E](https://doi.org/10.1016/0304-4203(91)90002-E)
- Erickson, B. E., and Helz, G. R., 2000, Molybdenum (VI) speciation in sulfidic waters: Stability and lability of thiomolybdates: *Geochimica et Cosmochimica Acta*, v. 64, n. 7, p. 1149–1158, [https://doi.org/10.1016/S0016-7037\(99\)00423-8](https://doi.org/10.1016/S0016-7037(99)00423-8)
- Ferdelman, T. G., ms, 1988, The distribution of sulfur, iron, manganese, copper and uranium in a salt marsh sediment core as determined by a sequential extraction method: Delaware, University of Delaware, MS thesis, 244 p.
- Ferrell, R. T., and Himmelblau, D. M., 1967, Diffusion coefficients of nitrogen and oxygen in water: *Journal of Chemical and Engineering Data*, v. 12, n. 1, p. 111–115, <https://doi.org/10.1021/jc60032a036>
- Forrest, J., and Newman, L., 1977, Silver-110 microgram sulfate analysis for the short time resolution of ambient levels of sulfur aerosol: *Analytical Chemistry*, v. 49, n. 11, p. 1579–1584, <https://doi.org/10.1021/ac50019a030>
- Gill, B. C., Lyons, T. W., Young, S. A., Kump, L. R., Knoll, A. H., and Saltzman, M. R., 2011, Geochemical evidence for widespread euxinia in the Later Cambrian ocean: *Nature*, v. 469, p. 80–83, <https://doi.org/10.1038/nature09700>
- Goldberg, T., Archer, C., Vance, D., Thamdrup, B., McAnena, A., and Poulton, S. W., 2012, Controls on Mo isotope fractionations in a Mn-rich anoxic marine sediment, Gullmar Fjord, Sweden: *Chemical Geology*, v. 296–297, p. 73–82, <https://doi.org/10.1016/j.chemgeo.2011.12.020>
- Goldhaber, M. B., Aller, R. C., Cochran, J. K., Rosenfeld, J. K., Martens, C. S., and Berner, R. A., 1977, Sulfate reduction, diffusion, and bioturbation in Long Island Sound sediments: Report of the FOAM Group: *American Journal of Science*, v. 277, n. 3, p. 193–237, <https://doi.org/10.2475/ajs.277.3.193>
- Green, M. A., and Aller, R. C., 1998, Seasonal patterns of carbonate diagenesis in nearshore terrigenous muds: Relation to spring phytoplankton bloom and temperature: *Journal of Marine Research*, v. 56, n. 5, p. 1097–1123, <https://doi.org/10.1357/002224098765173473>
- 2001, Early diagenesis of calcium carbonate in Long Island Sound sediments: Benthic fluxes of  $\text{Ca}^{2+}$

- and minor elements during seasonal periods of net dissolution: *Journal of Marine Research*, v. 59, n. 5, p. 769–794, <https://doi.org/10.1357/002224001762674935>
- Hardisty, D. S., Riedinger, N., Planavsky, N. J., Asael, D., Andr en, T., J rgensen, B. B., and Lyons, T. W., 2016, A Holocene history of dynamic water column redox conditions in the Landsort Deep, Baltic Sea: *American Journal of Science*, v. 316, n. 8, p. 713–745, <https://doi.org/10.2475/08.2016.01>
- Hayduk, W., and Laudie, H., 1974, Prediction of diffusion coefficients for nonelectrolytes in dilute aqueous solutions: *AIChE Journal*, v. 20, n. 3, p. 611–615, <https://doi.org/10.1002/aic.690200329>
- Helz, G. R., Miller, C. V., Charnock, J. M., Mosselmans, J. F. W., Patrick, R. A. D., Garner, C. D., and Vaughan, D. J., 1996, Mechanism of molybdenum removal from the sea and its concentration in black shales: EXAFS evidence: *Geochimica et Cosmochimica Acta*, v. 60, n. 19, p. 3631–3642, [https://doi.org/10.1016/0016-7037\(96\)00195-0](https://doi.org/10.1016/0016-7037(96)00195-0)
- Helz, G. R., Bura-Nakić, E., Mikc, N., and Ciglenečki, I., 2011, New model for molybdenum behavior in euxinic waters: *Chemical Geology*, v. 284, n. 3–4, p. 323–332, <https://doi.org/10.1016/j.chemgeo.2011.03.012>
- Henkel, S., Kasten, S., Poulton, S. W., and Staubwasser, M., 2016, Determination of the stable iron isotopic composition of sequentially leached iron phases in marine sediments: *Chemical Geology*, v. 421, p. 93–102, <https://doi.org/10.1016/j.chemgeo.2015.12.003>
- Johnston, D. T., Farquhar, J., and Canfield, D. E., 2007, Sulfur isotope insights into microbial sulfate reduction: *When microbes meet models*: *Geochimica et Cosmochimica Acta*, v. 71, n. 16, p. 3929–3947, <https://doi.org/10.1016/j.gca.2007.05.008>
- Johnston, D. T., Farquhar, J., Habicht, K. S., and Canfield, D. E., 2008, Sulphur isotopes and the search for life: Strategies for identifying sulphur metabolisms in the rock record and beyond: *Geobiology*, v. 6, n. 5, p. 425–435, <https://doi.org/10.1111/j.1472-4669.2008.00171.x>
- Johnston, D. T., Poulton, S. W., Goldberg, T., Sergeev, V. N., Podkovyrov, V., Vorob'eva, N. G., Bekker, A., and Knoll, A. H., 2012, Late Ediacaran redox stability and metazoan evolution: *Earth and Planetary Science Letters*, v. 335–336, p. 25–35, <https://doi.org/10.1016/j.epsl.2012.05.010>
- Kalil, E. K., and Goldhaber, M., 1973, A sediment squeezer for removal of pore waters without air contact: *Journal of Sedimentary Research*, v. 43, n. 2, p. 553–557, <https://doi.org/10.1306/74D727E8-2B21-11D7-8648000102C1865D>
- Kendall, B., Reinhard, C. T., Lyons, T. W., Kaufman, A. J., Poulton, S. W., and Anbar, A. D., 2010, Pervasive oxygenation along late Archaean ocean margins: *Nature Geoscience*, v. 3, p. 647–652, <https://doi.org/10.1038/ngeo942>
- Kostka, J. E., and Luther, G. W., III, 1994, Partitioning and speciation of solid phase iron in saltmarsh sediments: *Geochimica et Cosmochimica Acta*, v. 58, n. 7, p. 1701–1710, [https://doi.org/10.1016/0016-7037\(94\)90531-2](https://doi.org/10.1016/0016-7037(94)90531-2)
- Krishnaswami, S., Benninger, L. K., Aller, R. C., and Von Damm, K. L., 1980, Atmospherically-derived radionuclides as tracers of sediment mixing and accumulation in near-shore marine and lake sediments: Evidence from <sup>7</sup>Be, <sup>210</sup>Pb, and <sup>239,240</sup>Pu: *Earth and Planetary Science Letters*, v. 47, n. 3, p. 307–318, [https://doi.org/10.1016/0012-821X\(80\)90017-5](https://doi.org/10.1016/0012-821X(80)90017-5)
- Krishnaswami, S., Monaghan, M. C., Westrich, J., Bennett, J., and Turekian, K., 1984, Chronologies of sedimentary processes in sediments of the FOAM site, Long Island Sound, Connecticut: *American Journal of Science*, v. 284, n. 6, p. 706–733, <https://doi.org/10.2475/ajs.284.6.706>
- Lee, Y. J., and Lwiza, K., 2005, Interannual variability of temperature and salinity in shallow water: Long Island Sound, New York: *Journal of Geophysical Research: Oceans*, v. 110, <https://doi.org/10.1029/2004JC002507>
- Lee, Y. J., and Lwiza, K. M. M., 2008, Characteristics of bottom dissolved oxygen in Long Island Sound, New York: *Estuarine, Coastal and Shelf Science*, v. 76, n. 2, p. 187–200, <https://doi.org/10.1016/j.ejss.2007.07.001>
- Li, C., Love, G. D., Lyons, T. W., Fike, D. A., Sessions, A. L., and Chu, X., 2010, A stratified redox model for the Ediacaran ocean: *Science*, v. 328, n. 5974, p. 80–83, <https://doi.org/10.1126/science.1182369>
- Lyons, T. W., 1997, Sulfur isotopic trends and pathways of iron sulfide formation in upper Holocene sediments of the anoxic Black Sea: *Geochimica et Cosmochimica Acta*, v. 61, n. 16, p. 3367–3382, [https://doi.org/10.1016/S0016-7037\(97\)00174-9](https://doi.org/10.1016/S0016-7037(97)00174-9)
- Lyons, T. W., and Kashgarian, M., 2005, Paradigm Lost, Paradigm Found: *Oceanography*, v. 18, n. 2, p. 86–99, <https://doi.org/10.5670/oceanog.2005.44>
- Lyons, T. W., and Severmann, S., 2006, A critical look at iron paleoredox proxies: New insights from modern euxinic marine basins: *Geochimica et Cosmochimica Acta*, v. 70, n. 23, p. 5698–5722, <https://doi.org/10.1016/j.gca.2006.08.021>
- Lyons, T. W., Werne, J. P., Hollander, D. J., and Murray, R., 2003, Contrasting sulfur geochemistry and Fe/Al and Mo/Al ratios across the last oxic-to-anoxic transition in the Cariaco Basin, Venezuela: *Chemical Geology*, v. 195, n. 1–4, p. 131–157, [https://doi.org/10.1016/S0009-2541\(02\)00392-3](https://doi.org/10.1016/S0009-2541(02)00392-3)
- Malcolm, S., 1985, Early diagenesis of molybdenum in estuarine sediments: *Marine Chemistry*, v. 16, n. 3, p. 213–225, [https://doi.org/10.1016/0304-4203\(85\)90062-3](https://doi.org/10.1016/0304-4203(85)90062-3)
- Malinovsky, D., Baxter, D. C., and Rodushkin, I., 2007, Ion-specific isotopic fractionation of molybdenum during diffusion in aqueous solutions: *Environmental Science & Technology*, v. 41, p. 1596–1600, <https://doi.org/10.1021/es062000q>
- Marz, C., Poulton, S. W., Beckmann, B., Kuster, K., Wagner, T., and Kasten, S., 2008, Redox sensitivity of P cycling during marine black shale formation: Dynamics of sulfidic and anoxic, non-sulfidic bottom waters: *Geochimica et Cosmochimica Acta*, v. 72, n. 15, p. 3703–3717, <https://doi.org/10.1016/j.gca.2008.04.025>
- Marz, C., Poulton, S. W., Brumsack, H.-J., and Wagner, T., 2012, Climate-controlled variability of iron

- deposition in the Central Arctic Ocean (southern Mendeleev Ridge) over the last 130,000 years: *Chemical Geology*, v. 330–331, p. 116–126, <https://doi.org/10.1016/j.chemgeo.2012.08.015>
- McLennan, S. M., 2001, Relationships between the trace element composition of sedimentary rocks and upper continental crust: *Geochemistry, Geophysics, Geosystems*, v. 2, n. 4, <https://doi.org/10.1029/2000GC000109>
- McManus, J., Berelson, W. M., Severmann, S., Poulson, R. L., Hammond, D. E., Klinkhammer, G. P., and Holm, C., 2006, Molybdenum and uranium geochemistry in continental margin sediments: Paleoproxy potential: *Geochimica et Cosmochimica Acta*, v. 70, n. 5, p. 4643–4662, <https://doi.org/10.1016/j.gca.2006.06.1564>
- Miller, C. A., Peucker-Ehrenbrink, B., Walker, B. D., and Marcantonio, F., 2011, Re-assessing the surface cycling of molybdenum and rhenium: *Geochimica et Cosmochimica Acta*, v. 75, n. 22, p. 7146–7179, <https://doi.org/10.1016/j.gca.2011.09.005>
- Morford, J. L., and Emerson, S., 1999, The geochemistry of redox sensitive trace metals in sediments: *Geochimica et Cosmochimica Acta*, v. 63, n. 11–12, p. 1735–1750, [https://doi.org/10.1016/S0016-7037\(99\)00126-X](https://doi.org/10.1016/S0016-7037(99)00126-X)
- Morford, J. L., Martin, W. R., Kalnejais, L. H., François, R., Bothner, M., and Karle, I.-M., 2007, Insights on geochemical cycling of U, Re and Mo from seasonal sampling in Boston Harbor, Massachusetts, USA: *Geochimica et Cosmochimica Acta*, v. 71, n. 4, p. 895–917, <https://doi.org/10.1016/j.gca.2006.10.016>
- Morford, J. L., Martin, W. R., François, R., and Carney, C. M., 2009, A model for uranium, rhenium, and molybdenum diagenesis in marine sediments based on results from coastal locations: *Geochimica et Cosmochimica Acta*, v. 73, n. 10, p. 2938–2960, <https://doi.org/10.1016/j.gca.2009.02.029>
- Nameroff, T., Balistrieri, L. S., and Murray, J. W., 2002, Suboxic trace metal geochemistry in the eastern tropical North Pacific: *Geochimica et Cosmochimica Acta*, v. 66, n. 7, p. 1139–1158, [https://doi.org/10.1016/S0016-7037\(01\)00843-2](https://doi.org/10.1016/S0016-7037(01)00843-2)
- Owens, J. D., Lyons, T. W., Hardisty, D. S., Lowery, C. M., Lu, Z., Lee, B., and Jenkyns, H. C., 2017, Patterns of local and global redox variability during the Cenomanian–Turonian Boundary Event (Oceanic Anoxic Event 2) recorded in carbonates and shales from central Italy: *Sedimentology*, v. 64, n. 1, p. 168–185, <https://doi.org/10.1111/sed.12352>
- Pedersen, T. F., 1985, Early diagenesis of copper and molybdenum in mine tailings and natural sediments in Rupert and Holberg inlets, British Columbia: *Canadian Journal of Earth Sciences*, v. 22, p. 1474–1484, <https://doi.org/10.1139/e85-153>
- Peketi, A., Mazumdar, A., Joao, H., Patil, D., Usapkar, A., and Dewangan, P., 2015, Coupled C–S–Fe geochemistry in a rapidly accumulating marine sedimentary system: Diagenetic and depositional implications: *Geochemistry, Geophysics, Geosystems*, v. 16, n. 9, p. 2865–2883, <https://doi.org/10.1002/2015GC005754>
- Planavsky, N. J., McGoldrick, P., Scott, C. T., Li, C., Reinhard, C. T., Kelly, A. E., Chu, X., Bekker, A., Love, G. D., and Lyons, T. W., 2011, Widespread iron-rich conditions in the mid-Proterozoic ocean: *Nature*, v. 477, p. 448–451, <https://doi.org/10.1038/nature10327>
- Poulson, R. L., McManus, J., Severmann, S., and Berelson, W. M., 2009, Molybdenum behavior during early diagenesis: Insights from Mo isotopes: *Geochemistry, Geophysics, Geosystems*, v. 10, n. 6, <https://doi.org/10.1029/2008GC002180>
- Poulson, R. L., Siebert, C., McManus, J., and Berelson, W. M., 2006, Authigenic molybdenum isotope signatures in marine sediments: *Geology*, v. 34, n. 8, p. 617–620, <https://doi.org/10.1130/G22485.1>
- Poulton, S. W., and Canfield, D. E., 2005, Development of a sequential extraction procedure for iron: Implications for iron partitioning in continentally derived particulates: *Chemical Geology*, v. 214, n. 3–4, p. 209–221, <https://doi.org/10.1016/j.chemgeo.2004.09.003>
- 2011, Ferruginous conditions: A dominant feature of the ocean through Earth's history: *Elements*, v. 7, n. 2, p. 107–112, <https://doi.org/10.2113/gselements.7.2.107>
- Poulton, S. W., and Raiswell, R., 2002, The low-temperature geochemical cycle of iron: From continental fluxes to marine sediment deposition: *American Journal of Science*, v. 302, n. 9, p. 774–805, <https://doi.org/10.2475/ajs.302.9.774>
- Poulton, S. W., Fralick, P. W., and Canfield, D. E., 2004, The transition to a sulphidic ocean ~ 1.84 billion years ago: *Nature*, v. 431, p. 173–177, <https://doi.org/10.1038/nature02912>
- Raiswell, R., and Anderson, T. F., 2005, Reactive iron enrichment in sediments deposited beneath euxinic bottom waters: Constraints on supply by shelf recycling: *Geological Society, London, Special Publications*, v. 248, p. 179–194, <https://doi.org/10.1144/GSL.SP.2005.248.01.10>
- Raiswell, R., and Canfield, D. E., 1998, Sources of iron for pyrite formation in marine sediments: *American Journal of Science*, v. 298, n. 3, p. 219–245, <https://doi.org/10.2475/ajs.298.3.219>
- Raiswell, R., Buckley, F., Berner, R. A., and Anderson, T. F., 1988, Degree of pyritization of iron as a paleoenvironmental indicator of bottom-water oxygenation: *Journal of Sedimentary Research*, v. 58, n. 5, p. 812–819, <https://doi.org/10.1306/212F8E72-2B24-11D7-8648000102C1865D>
- Raiswell, R., Canfield, D. E., and Berner, R. A., 1994, A comparison of iron extraction methods for the determination of degree of pyritization and the recognition of iron-limited pyrite formation: *Chemical Geology*, v. 111, n. 1–4, p. 101–110, [https://doi.org/10.1016/0009-2541\(94\)90084-1](https://doi.org/10.1016/0009-2541(94)90084-1)
- Raiswell, R., Vu, H. P., Brinza, L., and Benning, L. G., 2010, The determination of labile Fe in ferrihydrite by ascorbic acid extraction: Methodology, dissolution kinetics and loss of solubility with age and de-watering: *Chemical Geology*, v. 278, p. 70–79.
- Raiswell, R., Hardisty, D. S., Lyons, T. W., Canfield, D. E., Owens, J. D., Planavsky, N. J., Poulton, S. W., and Reinhard, C. T., 2018, The iron paleoredox proxies: A guide to the pitfalls, problems and proper practice: *American Journal of Science*, v. 318, n. 5, p. , <https://doi.org/10.2475/05.2018.03>
- Raven, M. R., Sessions, A. L., Fischer, W. W., and Adkins, J. F., 2016, Sedimentary pyrite  $\delta^{34}\text{S}$  differs from

- porewater sulfide in Santa Barbara Basin: Proposed role of organic sulfur: *Geochimica et Cosmochimica Acta*, v. 186, p. 120–134, <https://doi.org/10.1016/j.gca.2016.04.037>
- Reed, D. C., Slomp, C. P., and Gustafsson, B. G., 2011, Sedimentary phosphorus dynamics and the evolution of bottom-water hypoxia: A coupled benthic–pelagic model of a coastal system: *Limnology and Oceanography*, v. 56, n. 3, p. 1075–1092, <https://doi.org/10.4319/lom.2011.56.3.1075>
- Reinhard, C. T., Raiswell, R., Scott, C., Anbar, A. D., and Lyons, T. W., 2009, A late Archean sulfidic sea stimulated by early oxidative weathering of the continents: *Science*, v. 326, n. 5953, p. 713–716, <https://doi.org/10.1126/science.1176711>
- Riedinger, N., Brunner, B., Krastel, S., Arnold, G. L., Wehrmann, L. M., Formolo, M. J., Beck, A., Bates, S. M., Henkel, S., Kasten, S., and Lyons, T. W., 2017, Sulfur cycling in an iron oxide-dominated, dynamic marine depositional system: The Argentine continental margin: *Frontiers in Earth Science*, article 33, <https://doi.org/10.3389/feart.2017.00033>
- Scholz, F., Hensen, C., Noffke, A., Rohde, A., Liebetrau, V., and Wallmann, K., 2011, Early diagenesis of redox-sensitive trace metals in the Peru upwelling area—response to ENSO-related oxygen fluctuations in the water column: *Geochimica et Cosmochimica Acta*, v. 75, n. 22, p. 7257–7276, <https://doi.org/10.1016/j.gca.2011.08.007>
- Scholz, F., Severmann, S., McManus, J., and Hensen, C., 2014a, Beyond the Black Sea paradigm: The sedimentary fingerprint of an open-marine iron shuttle: *Geochimica et Cosmochimica Acta*, v. 127, p. 368–380, <https://doi.org/10.1016/j.gca.2013.11.041>
- Scholz, F., Severmann, S., McManus, J., Noffke, A., Lomnitz, U., and Hensen, C., 2014b, On the isotope composition of reactive iron in marine sediments: Redox shuttle versus early diagenesis: *Chemical Geology*, v. 389, p. 48–59, <https://doi.org/10.1016/j.chemgeo.2014.09.009>
- Scholz, F., Löscher, C. R., Fiskal, A., Sommer, S., Hensen, C., Lomnitz, U., Wuttig, K., Göttlicher, J., Kossel, E., Steininger, R., and Canfield, D. E., 2016, Nitrate-dependent iron oxidation limits iron transport in anoxic ocean regions: *Earth and Planetary Science Letters*, v. 454, p. 272–281, <https://doi.org/10.1016/j.epsl.2016.09.025>
- Scholz, F., Siebert, C., Dale, A. W., and Frank, M., 2017, Intense molybdenum accumulation in sediments underneath a nitrogenous water column and implications for the reconstruction of paleo-redox conditions based on molybdenum isotopes: *Geochimica et Cosmochimica Acta*, v. 213, p. 400–417, <https://doi.org/10.1016/j.gca.2017.06.048>
- Scott, C., and Lyons, T. W., 2012, Contrasting molybdenum cycling and isotopic properties in euxinic versus non-euxinic sediments and sedimentary rocks: Refining the paleoproxies: *Chemical Geology*, v. 324–325, p. 19–27, <https://doi.org/10.1016/j.chemgeo.2012.05.012>
- Scott, C., Lyons, T. W., Bekker, A., Shen, Y., Poulton, S. W., Chu, X., and Anbar, A. D., 2008, Tracing the stepwise oxygenation of the Proterozoic ocean: *Nature*, v. 452, p. 456–459, <https://doi.org/10.1038/nature06811>
- Scott, C. T., Bekker, A., Reinhard, C. T., Schnetger, B., Krapež, B., Rumble, D., III, and Lyons, T. W., 2011, Late Archean euxinic conditions before the rise of atmospheric oxygen: *Geology*, v. 39, n. 2, p. 119–122, <https://doi.org/10.1130/G31571.1>
- Seeberg-Elverfeldt, J., Schlüter, M., Feseker, T., and Kölling, M., 2005, Rhizon sampling of porewaters near the sediment–water interface of aquatic systems: *Limnology and oceanography: Methods*, v. 3, n. 8, p. 361–371, <https://doi.org/10.4319/lom.2005.3.361>
- Severmann, S., Lyons, T. W., Anbar, A., McManus, J., and Gordon, G., 2008, Modern iron isotope perspective on the benthic iron shuttle and the redox evolution of ancient oceans: *Geology*, v. 36, n. 6, p. 487–490, <https://doi.org/10.1130/G24670A.1>
- Severmann, S., McManus, J., Berelson, W. M., and Hammond, D. E., 2010, The continental shelf benthic iron flux and its isotope composition: *Geochimica et Cosmochimica Acta*, v. 74, n. 14, p. 3984–4004, <https://doi.org/10.1016/j.gca.2010.04.022>
- Shimmield, G. B., and Price, N. B., 1986, The behaviour of molybdenum and manganese during early sediment diagenesis—offshore Baja California, Mexico: *Marine Chemistry*, v. 19, n. 3, p. 261–280, [https://doi.org/10.1016/0304-4203\(86\)90027-7](https://doi.org/10.1016/0304-4203(86)90027-7)
- Sperling, E. A., Wolock, C. J., Morgan, A. S., Gill, B. C., Kunzmann, M., Halverson, G. P., Macdonald, F. A., Knoll, A. H., and Johnston, D. T., 2015, Statistical analysis of iron geochemical data suggests limited late Proterozoic oxygenation: *Nature*, v. 523, p. 451–454, <https://doi.org/10.1038/nature14589>
- Sundby, B., Martinez, P., and Gobeil, C., 2004, Comparative geochemistry of cadmium, rhenium, uranium, and molybdenum in continental margin sediments: *Geochimica et Cosmochimica Acta*, v. 68, n. 11, p. 2485–2493, <https://doi.org/10.1016/j.gca.2003.08.011>
- Tarhan, L. G., Droser, M. L., Planavsky, N. J., and Johnston, D. T., 2015, Protracted development of bioturbation through the early Palaeozoic Era: *Nature Geoscience*, v. 8, p. 865–869, <https://doi.org/10.1038/ngeo2537>
- Taylor, S. R., and McLennan, S. M., 1995, The geochemical evolution of the continental crust: *Reviews of Geophysics*, v. 33, p. 241–265, <https://doi.org/10.1029/95RG00262>
- Turekian, K. K., and Wedepohl, K. H., 1961, Distribution of the elements in some major units of the earth's crust: *Geological Society of America Bulletin*, v. 72, n. 2, p. 175–192, [https://doi.org/10.1130/0016-7606\(1961\)72\[175:DOTAIS\]2.0.CO;2](https://doi.org/10.1130/0016-7606(1961)72[175:DOTAIS]2.0.CO;2)
- Wagner, M., Chappaz, A., and Lyons, T. W., 2017, Molybdenum speciation and burial pathway in weakly sulfidic environments: Insights from XAFS: *Geochimica et Cosmochimica Acta*, v. 206, p. 18–29, <https://doi.org/10.1016/j.gca.2017.02.018>
- Wallace, R. B., Baumann, H., Gear, J. S., Aller, R. C., and Gobler, C. J., 2014, Coastal ocean acidification: The other eutrophication problem: *Estuarine, Coastal and Shelf Science*, v. 148, p. 1–13, <https://doi.org/10.1016/j.ecss.2014.05.027>
- Wang, D., Aller, R. C., and Sañudo-Wilhelmy, S. A., 2011, Redox speciation and early diagenetic behavior of

- dissolved molybdenum in sulfidic muds: *Marine Chemistry*, v. 125, n. 1–4, p. 101–107, <https://doi.org/10.1016/j.marchem.2011.03.002>
- Wehrmann, L. M., Formolo, M. J., Owens, J. D., Raiswell, R., Ferdelman, T. G., Riedinger, N., and Lyons, T. W., 2014, Iron and manganese speciation and cycling in glacially influenced high-latitude fjord sediments (West Spitsbergen, Svalbard): Evidence for a benthic recycling-transport mechanism: *Geochimica et Cosmochimica Acta*, v. 141, p. 628–655, <https://doi.org/10.1016/j.gca.2014.06.007>
- Westrich, J. T., ms, 1983, The consequences and controls of bacterial sulfate reduction in marine sediments: New Haven, Connecticut, Yale University, Ph. D. thesis, 530 p.
- Westrich, J. T., and Berner, R. A., 1988, The effect of temperature on rates of sulfate reduction in marine sediments: *Geomicrobiology Journal*, v. 6, n. 2, p. 99–117, <https://doi.org/10.1080/01490458809377828>
- Wijsman, J. W. M., Middelburg, J. J., and Heip, C. H. R., 2001, Reactive iron in Black Sea sediments: Implications for iron cycling: *Marine Geology*, v. 172, n. 3–4, p. 167–180, [https://doi.org/10.1016/S0025-3227\(00\)00122-5](https://doi.org/10.1016/S0025-3227(00)00122-5)
- Zheng, Y., Anderson, R. F., van Geen, A., and Kuwabara, J., 2000, Authigenic molybdenum formation in marine sediments: A link to pore water sulfide in the Santa Barbara Basin: *Geochimica et Cosmochimica Acta*, v. 64, n. 25, p. 4165–4178, [https://doi.org/10.1016/S0016-7037\(00\)00495-6](https://doi.org/10.1016/S0016-7037(00)00495-6)
- Zhou, X., Jenkyns, H. C., Lu, W., Hardisty, D. S., Owens, J. D., Lyons, T. W., and Lu, Z., 2017, Organically bound iodine as a bottom-water redox proxy: Preliminary validation and application: *Chemical Geology*, v. 457, p. 95–106, <https://doi.org/10.1016/j.chemgeo.2017.03.016>
- Zhu, M.-X., Hao, X.-C., Shi, X.-N., Yang, G.-P., and Li, T., 2012, Speciation and spatial distribution of solid-phase iron in surface sediments of the East China Sea continental shelf: *Applied Geochemistry*, v. 27, n. 4, p. 892–905, <https://doi.org/10.1016/j.apgeochem.2012.01.004>
- Zhu, M.-X., Huang, X.-L., Yang, G.-P., and Chen, L.-J., 2015, Iron geochemistry in surface sediments of a temperate semi-enclosed bay, North China: *Estuarine, Coastal and Shelf Science*, v. 165, p. 25–35, <https://doi.org/10.1016/j.ecss.2015.08.018>